The Climatic and Hydrologic History of Southern Nevada During the Late Quaternary

---

U.S. GEOLOGICAL SURVEY

Open-File Report 98–635

Prepared in cooperation with the
NEVADA OPERATIONS OFFICE
U.S. DEPARTMENT OF ENERGY
(Interagency Agreement DE-AI08-97NV12033)

DISCLAIMER

DISCLAIMER

The Climatic and Hydrologic History of Southern Nevada During the Late Quaternary

By R.M. Forester[1], J.P. Bradbury[2], C. Carter[3], A.B. Elvidge-Tuma[4], M.L. Hemphill[5], S.C. Lundstrom[1], S.A. Mahan[1], B.D. Marshall[1], L.A. Neymark[6], J.B. Paces[1], S.E. Sharpe[7], J.F. Whelan[1], and P.E. Wigand[8]

[1]USGS, Denver, CO, [2]USGS, Denver, CO (retired), [3]USGS, Menlo Park, CA (retired), [4]1725 S. McCarren, Reno, NV, [5]Department of Anthropology, Washington State University, Pullman, WA, [6]Pacific Western Technologies Ltd., Lakewood, CO, [7]Nevada Division of Water Planning, 1550 E. College Parkway, Suite 142, Carson City, NV, [8]2210 Seneca Drive, Reno, NV

U.S. GEOLOGICAL SURVEY

Open-File Report 98–635

Prepared in cooperation with the
NEVADA OPERATIONS OFFICE
U.S. DEPARTMENT OF ENERGY
(Interagency Agreement DE-AI08-97NV12033)

Denver, Colorado
1999

U.S. DEPARTMENT OF THE INTERIOR
BRUCE BABBITT, Secretary

U.S. GEOLOGICAL SURVEY
Charles G. Groat, Director

For additional information write to:

Chief, Earth Science Investigations Program
Yucca Mountain Project Branch
U.S. Geological Survey
Box 25046, Mail Stop 421
Denver Federal Center
Denver, CO 80225-0046

Copies of this report can be purchased from:

U.S. Geological Survey
Information Services
Box 25286
Federal Center
Denver, CO 80225

Long Climate Records 10
Devils Hole 10
Owens Lake 11
Climate and Hydrologic Setting 13
Climate Linkage to Owens Lake Chemistry and Paleontology 13
Core Stratigraphy 15
Lithostratigraphy 15
Chronostratigraphy 15
Owens Lake Diatom Record 15
Diatom Analysis 15
Methods 15
Paleohydrologic History of Owens Lake—The Diatom Record 16
Owens Lake Ostracode Record 16
Ostracode Methods 16
Paleolimnological History of Owens Lake—The Ostracode Record 16
Correlation of Owens Lake Paleolimnology and Oxygen Isotope Records 18
Other Data Sets 21
Conclusions 21
Lakes, Playas, and Marshes 21
Introduction 21
Corn Creek Flat (Main) Section OCI–11 22
Terrestrial Vegetation Records 24
Introduction 24
Modern Climate and Vegetation of Southern Nevada Deserts 24
Results and Discussion 24
Limber Pine 27
White Fir 27
Fossil Record 27
Spatial and Chronological Continuity of Data 27
Timing 27
Elevational Displacement 27
Environmental Parameters 27
Pleistocene Wet Periods 32
Conclusions and Summary 32
Conclusions 32
Summary 33
Comparison of Aquatic and Terrestrial Records 33
Late Quaternary History of Surficial Deposits at Yucca Mountain—A Record of Geomorphic and Surface Hydrologic Response to Climate Change 33
The Fluvial Record of Fortymile Wash 34
Hydroclimatic Implications of Fortymile Wash History 35
Quaternary Hydrology 36
Stable Isotope Geochemistry and Mineralogy 36
Secondary Mineral Parageneses 36
Isotopic Geochemistry of Unsaturated-Zone Secondary Calcite 37

[illegible]

3. Generalized depiction of a three-celled circulation pattern of the Northern Hemisphere 5

4–10. Graphs showing:

4. Common orbital parameters, eccentricity versus precession, and precession versus insolation plotted against a time axis 6

5. Comparison of the delta oxygen-18 record from Devils Hole to other climate records (SPECMAP and Vostok), as well as with the insolation plotted against a time axis 12

6. Relative abundance of various kinds of diatoms from Owens Lake, California 16

7. Relative abundance of various ostracode species found in Owens Lake, California, plotted against a generalized lithologic column 17

8. Comparison of the freshwater planktic diatom stratigraphic distribution from Owens Lake to the SPECMAP and Devils Hole records 19

9. Comparison of key ostracode species stratigraphic profiles from Owens Lake to the SPECMAP and Devils Hole climate records 20

10. Comparison of the stratigraphic distribution of key kinds of ostracodes to their stratigraphic record 23

11. Index map showing Southern Nevada woodrat-midden localities mentioned in this study identified 26

12. Graph showing chronologic plot of the elevational distribution of directly dated limber pine macrofossils from ancient woodrat middens from a 200-km radius around Yucca Mountain; radiocarbon dates on limber pine for this study plotted as a normal distribution at three standard deviations around the mean; and radiocarbon dates on limber pine for other studies plotted as a normal distribution at three standard deviations around the mean 28

13. Chronologic plot of the elevational distribution of directly dated white fir macrofossils from ancient woodrat middens from a 200-km radius around Yucca Mountain; radiocarbon dates on white fir for this study plotted as a normal distribution at three standard deviations around the mean; and radiocarbon dates on white fir for other studies plotted as a normal distribution at three standard deviations around the mean 29
14. Graphs showing the distribution of directly dated limber pine, white fir, Utah juniper, and pinyon pine through time and by elevation from ancient woodrat middens from a 200-km radius around Yucca Mountain 30
15. Graph showing plot of delta carbon-13 and delta oxygen-18 values of calcite versus depth within the unsaturated zone 37
16. Histogram showing the distribution of unsaturated-zone secondary calcite delta carbon-13 values 38
17. Graph showing strontium isotopic composition of calcite deposited at Devils Hole spring as a function of age 40
18. Graph showing strontium-87/86 ratios in calcites from various core holes as a function of depth relative to the depth of the water table in the core holes sampled 41
19. Schematic model for the strontium data on the pedogenic carbonate system 42
20. Histograms of apparent radiocarbon and thorium-230/uranium ages determined from calcites and opals from the Exploratory Studies Facility 45
21. Location map showing paleodischarge deposits 48
22. Map showing ages determined by thorium-230/uranium, radiocarbon, and thermoluminescence methods for samples from paleodischarge sites 49
23. Graph showing stable carbon and oxygen isotopic compositions of carbonates from the paleodischarge deposits that are the focus of this report plotted with different symbols representing each of the five sites 50
24. Map showing location of wells and springs analyzed for delta strontium-87 from waters 54

TABLES

1. Modern vegetation distributions within the Yucca Mountain area 25
2. Plant contents of radiocarbon-dated middens at key localities around southern Nevada 31
3. Characteristic isotopic compositions of paleodischarge deposits, waters, and rocks representing possible source materials 53
4. Matrix of possible hydrogenic sources and their compatibility with observed data from paleodischarge sites..... 55

CONVERSION FACTORS, VERTICAL DATUM, AND ABBREVIATIONS

Table 1:

Multiply	By	To obtain
centimeter (cm)	0.3937	inch
centimeter per thousand years (cm/ky)	0.3937	inch per thousand years
gram (g)	0.03527	ounce
kilometer (km)	0.6214	mile
meter (m)	3.281	foot
meter per year (m/yr)	3.281	foot per year
milligram (mg)	2.2×10^{-6}	pound
milligram per liter (mg/L)	1	part per million (ppm)
millimeter (mm)	0.03937	inch
square kilometer (km^2)	0.3861	square mile

Temperature in degrees Celsius (°C) may be converted to degrees Fahrenheit (°F) as follows:

$$°F = (1.8 \times °C) + 32$$

ADDITIONAL ABBREVIATIONS

millions of years (My)
millions of years before present (Ma)
thousand years before present (ka)
thousands of years (ky)

Sea level: In this report, "sea level" refers to the National Geodetic Vertical Datum of 1929 (NGVD of 1929)—a geodetic datum derived from a general adjustment of the first-order level nets of both the United States and Canada, formerly called Sea Level Datum of 1929.

[illegible] sion) that determine insolation. Orbital properties and the resulting insolation values can be calculated for the past and the future, so estimates of future conditions can be made by comparison to comparable conditions in the past. The major, insolation-controlled climate cycle is 400,000 years in duration with subcycles of approximately 100,000 years. Changes in insolation are closely correlated with the major features of global climate change, such as the growth and retreat of continental ice sheets. The anticipated change in insolation during the next 100,000 years resembles change in insolation during the period from 400,000 to 300,000 years before the present.

The Devils Hole isotopic climate record shows that regional climate in southern Nevada changed in concert with global climate change, and long sedimentary records from basins, such as Owens Lake, provide an estimate of the character, magnitude, and frequency of local climate change. These records, therefore, link changes in insolation to a climate response in the Yucca Mountain area. Climate data collected from cores taken in the Owens Lake Basin show that the [illegible] 10,000 years before the present) appear to have been wetter and colder than the glacial interval from about 400,000 to 350,000 years before the present, which may serve as an analog for the next glacial period. Substantiation of the latter observation with additional analyses would be a significant finding for the probable performance of a potential repository, at least from a climate perspective.

Interpretation of plant macrofossils found in woodrat middens near Yucca Mountain indicates that mean annual precipitation varied during the last wet period 40,000 to 10,000 years ago, but precipitation was typically as much as twice the modern mean annual precipitation value. In particular, the midden data show short, century- to millennial-scale episodes when white fir moved to lower elevations. During those episodes, mean annual precipitation was probably greater than twice modern mean values. The variation of mean annual precipitation remains to be estimated, but given the diversity of dry and wet plant types within various middens, the variation in mean annual precipitation was likely quite large. Present mean annual precipitation at Yucca Mountain is about 15 cm. Episodes without white

fluvial deposits in and around Fortymile Wash show a response to past-climate change. Alluvial and fluvial sediments were deposited during the wetter phases of interglacial periods and periods of transitional climates when infrequent but large storms eroded the hillslopes, including those of Yucca Mountain. Incision of those sediments occurred during cooler and wetter climate phases when hillslopes, which were stabilized by vegetation, supplied little sediment to the regular flow in Fortymile Wash. Deposition (drier climate) of sediment in the wash occurred from about 120,000 to about 50,000 years ago, and incision (wetter climate) occurred after this period and likely before the last glacial maxima period, about 18,000 radiocarbon years before the present.

Geochronologic, isotopic, geochemical, and petrographic studies of calcite and opal minerals precipitated within fractures inside Yucca Mountain provide a direct means of comparing past regional climates to changes in infiltration, percolation, and recharge within the unsaturated zone. Calcite and opal formation within the unsaturated zone (specifically beneath Yucca Mountain), based on stable carbon and oxygen isotopes and radiogenic strontium

Wells Diatomite 20 km south of Yucca Mountain and paleowetland deposits near the Amargosa River show that discharge occurred between about 40,000 and 8,000 years before the present. The discharge, at least in part, came from the regional aquifer when the water tables rose to a maximum of about 100 m above present levels, as indicated from the depth to regional ground water at the Lathrop Wells diatomite site.

INTRODUCTION

Understanding how future climate change may affect the hydrologic-environment of a potential high-level nuclear-waste repository at Yucca Mountain, Nevada, during its expected life span is the primary purpose of the climate studies. Study of long-term paleoclimate and paleohydrology provides a way to understand potential climatic and hydrologic variability on a time scale that is relevant to high-level nuclear waste isolation.

The present climate and hydrology of the Yucca Mountain, Nevada, area (figs. 1, 2, and 3) are coupled together as part of a long-term millennial-scale product of continuous, generally cyclical, climate change (fig. 4). The climate system responds to numerous short-term forcing functions, such as

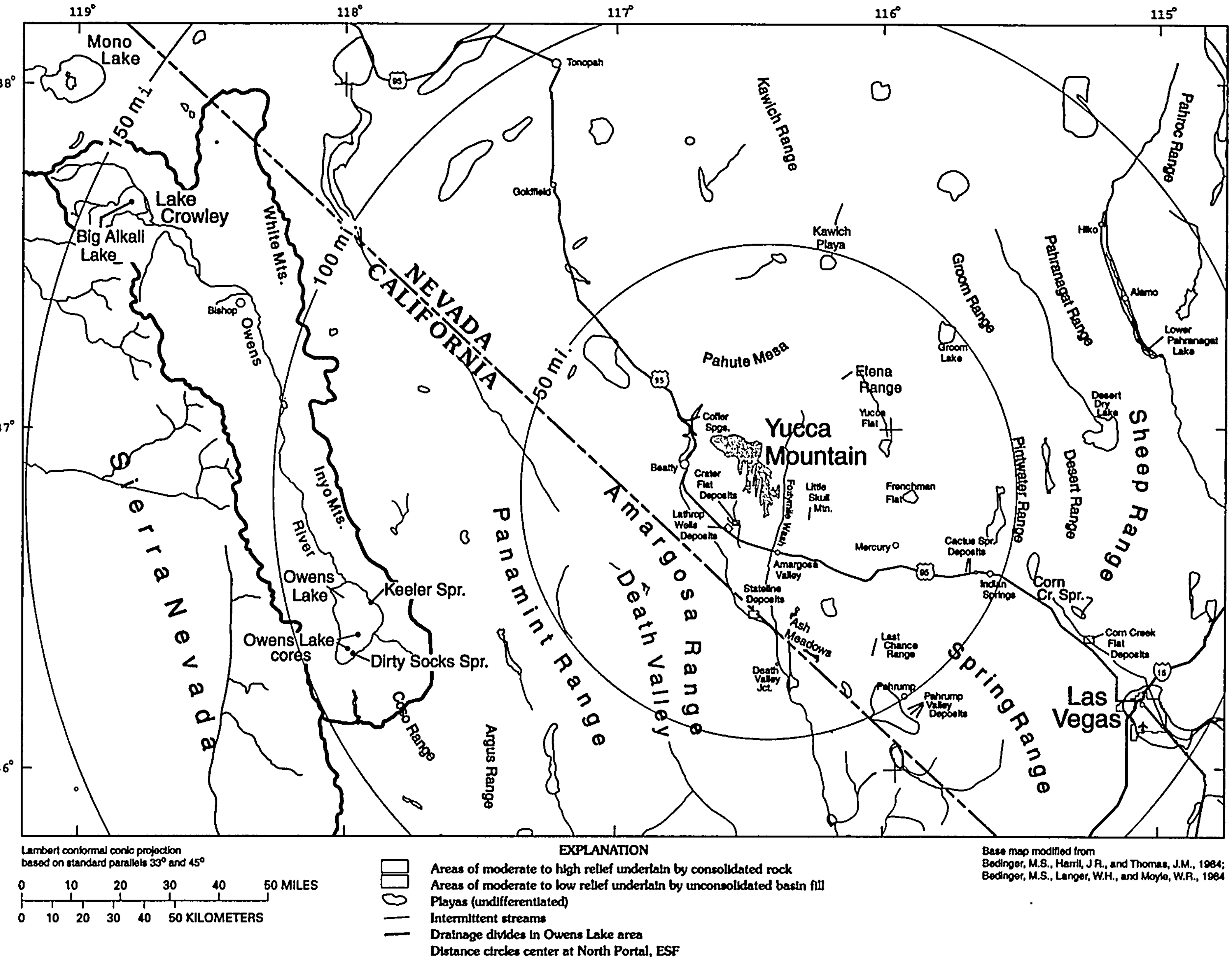

Figure 1. Key study sites near Yucca Mountain. See figure 2 for a detailed map of selected sites.

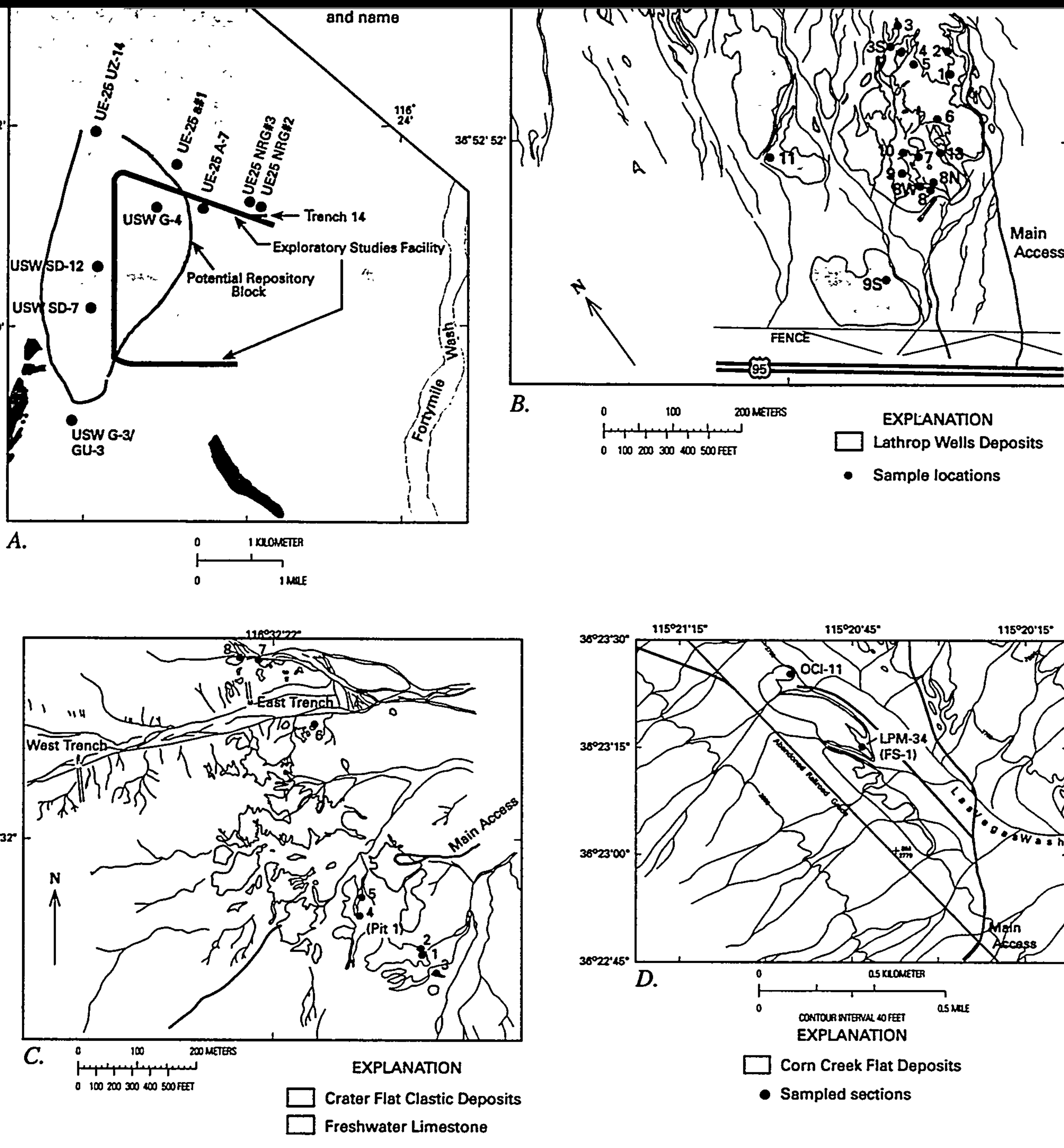

Figure 2. Maps of (*A*) southeastern Yucca Mountain showing potential repository site, sample boreholes, and Exploratory Studies Facility; (*B*) outcrop area of Lathrop Wells deposits showing sample localities; (*C*) studied outcrops in southeastern Crater Flat showing sample localities; and (*D*) parts of outcrop area of and sample localities in the Corn Creek Flats deposits.

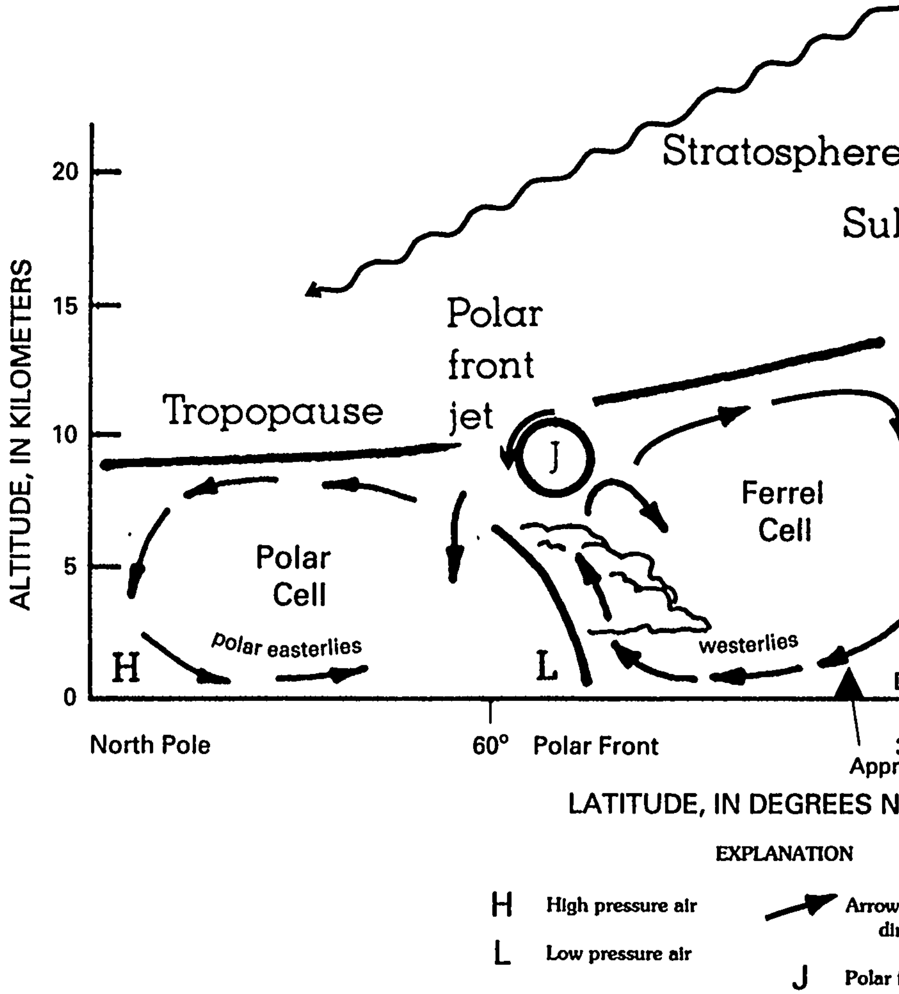

Figure 3. Generalized depiction of a three-celled circulation pattern of the Northern Hemis
filled triangle. Climate change results in expansion and contraction of the three major circu
example, the Polar cell expands and the Ferrel cell contracts (modified from Ahrens, 1985

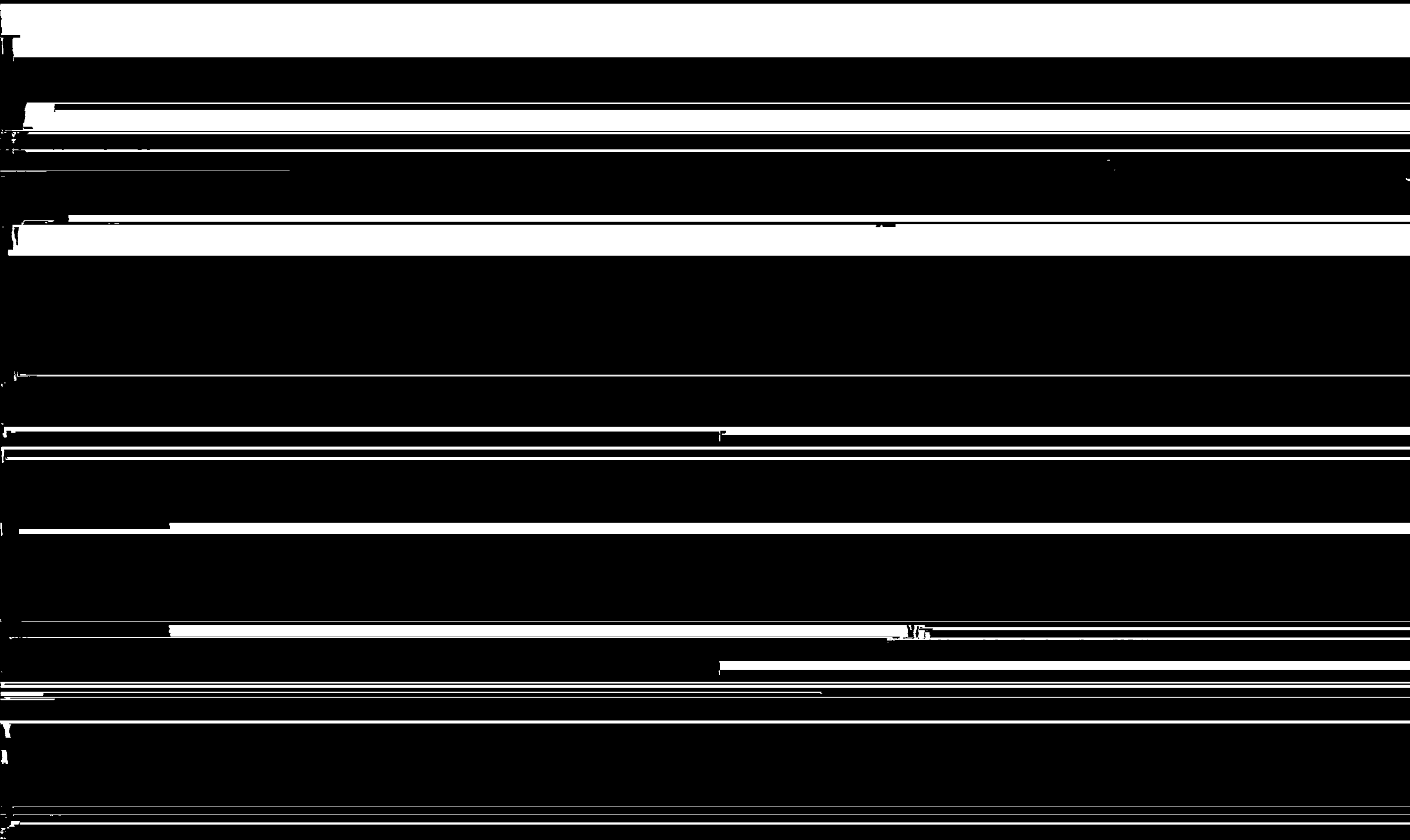

Figure 4. Common orbital parameters verus time. (A) Eccentricity relative to precession vs. time; (B) Summer insolation at 65°north latitude relative to precession vs. time; (C) Summer insolation at 30°north latitude vs. time for both past and future; (D) Detail enlargement of superposed segments from (C). Notice the importance of eccentricity on precesion (A) and the relation between precession and insolation; (B) Notice the similarity of insolation from about 400 to 300 ka versus that for the next 100 ky in the future, Berger and Loutre, 1991.

changes in insolation appear to be especially important correlates of climate change. In recent Earth history (the past 2 million years before the present or 2 Ma), changes in insolation are correlated with glacial and interglacial periods, with the glacial intervals being resident about 80 percent of the time. Climate also responds to very long-term forcing functions, over hundreds of thousands to millions of years, such as those related to continental drift or regional tectonics. As these very long-term forcing functions change, so does the mean millennial-scale character of climate. Regional hydrology, because it is coupled to climate, must respond to and change with climate. Thus, the millennial-scale characteristics of regional hydrology may be very different from those observed and measured over a short periods of time (decades to centuries). For example, southern Nevada regional-aquifer recharge was much higher during the last glacial period 40,000 to 10,000 years before the present, (40 to 10ka) than it is today (Benson and Kleiforth, 1989).

Evaluation of both past and future hydrologic characteristics of the potential high-level waste repository at Yucca Mountain cannot be based solely on modern hydrological studies. Although present-day studies reveal key characteristics details of the hydrological system, such as zones of infiltration, they cannot evaluate the characteristics of that system when major climate-system features, such as mean annual temperature (MAT), mean annual precipitation (MAP), and seasonal distributions of temperature and precipitation were different. The long-term millennial-scale properties of the climate and hydrologic system are the subject of this report.

CENTRAL HYPOTHESIS

Future climate patterns at Yucca Mountain may be estimated by understanding the processes that link climate and hydrological change to the cyclic variation in the Earth's insolation. Change in insolation is an important correlate with change in the climate system on a millennial scale. Interpretation and dating of past climatic and hydrologic changes in the vicinity of Yucca Mountain provide a linkage with past orbital those of past periods with similar insolation.

Climate responds to forcing functions that operate on all time scales from a year or less to millions of years. Short-term forcing functions involve factors, such as variability of solar output, of ocean/atmosphere heat exchange, such as the El Niño Southern Oscillation (ENSO), of volcanic eruptions, and of human-caused global warming. Long-term (million-year) forcing functions involve factors, such as continental drift, tectonics, and changes in ocean configuration. Change in Earth orbital characteristics occur on a millennial scale. Nonetheless, many factors must contribute to climate change, and the forcing functions likely operate on all time scales. As a consequence, future climate on the millennial scale almost certainly will not exactly repeat the past. Assuming that long-term Earth-based forcing functions, such as tectonics or ocean land configurations, remain relatively constant, however, changes in insolation should provide the timing for most future climate change for the next 100 millennia. That is, the characteristics of past climate cycles, within the confines of long-term Earth-based forcing functions, may repeat in the future and therein provide a basis to forecast future climate.

Present-day climate operates within a seasonal range of insolation values within which the influence of short-term forcing functions plays a key role. As the seasonal range of insolation changes, however, the short-term forcing functions, which are important at human scales, have no consistent bearing on the nature of future climate operating within other ranges of insolation values. Short-term forcing functions that operate in future climate states will perturb them in some way, just as they do the modern state, however. Similarly, because modern-day hydrology is linked strongly to modern-day climate, future hydrology cannot be estimated by studying only present hydrology or the hydrology at any particular time.

Because past climate and hydrology cannot be measured directly, proxy data must be interpreted in terms of climate or hydrology. Past climatic and hydrologic proxies typically come from fossil and isotopic data. Understanding the relation between an organism, which leaves a fossil record, and climate allows interpretation of past climate from fossils. Because the survival of any population relies on many biotic and abiotic factors other than climate, a particular biologic proxy may not reflect past climate in exactly the same way as another biotic proxy. Extraction of a climate signal from multiple proxies can produce a more realistic composite picture of past climate. In this study, the fossil data include plant macrofossils from woodrat middens, pollen, molluscs, ostracodes, diatoms, and fossil mammals.

Carbon, oxygen, strontium, and uranium isotopes offer additional climate and hydrological information. Isotopes reflect the characteristics of past surface and ground waters and provide insights into climate dynamics. More significantly, isotopic data provide information about percolating waters in the unsaturated zone (UZ) and ground waters in the saturated zone (SZ) and, hence, the linkage between the past climate and past hydrology.

The fossil and isotopic data are supported further by petrographic data collected from calcite and opaline vein fillings within Yucca Mountain, as well as from ground-water discharge deposits that occur down the flow gradient and from alluvial, fluvial, eolian, pedogenic, and related deposits on and near the mountain.

CAUSATION AND NATURE OF CLIMATE AND HYDROLOGICAL CHANGE IN SOUTHERN NEVADA—THE PRESENT AND PAST CLIMATE SYSTEM

Modern-Day Climate

Global climate may be thought of as the consequence of the atmosphere's attempt to balance a heat budget that is perpetually out of balance. Heat transport takes place in the oceans and the atmosphere. Throughout the year, the tropics receive more heat than the poles, demanding that the excess tropical heat moves toward the polar deficit.

Atmospheric heat transport from the tropics begins with rising air that moves poleward in the upper troposphere (lowest layer of the atmosphere), where it cools and typically sinks around 30° to 35°N latitude (fig. 3). Air flowing southward in the upper troposphere also descends in this region. The barometric pressure of the descending air rises near the Earth's surface and its relative humidity falls, creating a belt of hot deserts at 30 to 35°N latitude around the Earth. Some of the air within the hot desert belt flows back toward the Equator in the lower troposphere forming the subtropical easterlies (fig. 3). The huge atmospheric cell created by flow from and back to the Equator is called the Hadley cell. Other air from the desert belt flows poleward, creating a wind system known as the westerlies. The warm westerlies eventually meet cold, dense, southward-moving polar air within a seasonally variable geographic band. As the air masses meet, the warm air rises and moves from west to east along a sinuous front, called the polar front or the westerly storm track (fig. 3). The polar front exists as interfingering masses of polar and westerly air. An advancing cold front occurs when polar air displaces westerly air, and an advancing warm front typically occurs as westerly air moves over polar air. The net upward motion of air along the polar front produces an upper tropospheric air flow towards the pole and the Equator. The atmospheric cell, defined by the westerlies at its base, is referred to as a Ferrel cell. At the pole, cold upper-atmospheric air sinks, forming dense, dry, cold air in the lower troposphere that flows equatorward, creating the arctic easterlies (fig. 3). The southern edge of the arctic easterlies rise as they approach the westerlies forming a series of polar low pressure cells. The air-mass boundary between the northern cold air and the westerlies is the polar front, which is where the polar jet-stream resides. The atmospheric cell defined by arctic and polar air is typically referred to as a Polar cell.

The strong contrasts in air pressure and temperature between the Hadley, Ferrel, and Polar cells produce a focused, high-velocity air stream at their upper atmospheric boundaries called a jet stream. The polar jet, which is the stronger of the two, resides between the Polar and Ferrel cells, whereas the subtropical jet resides between the Ferrel and Hadley cells.

The perpetual input of excess heat to the tropics maintains the circulation described above. The relative positions and strengths of air movement within the three cells changes seasonally as the Northern and Southern Hemispheres warm or cool. The Hadley and Arctic cells, along their northern and southern edges, respectively, have time averaged large, relatively stable and geographically limited air masses whose properties such as water-vapor content, temperature, and barometric pressure persist for most or all of the year. Some of these air masses are named and include energize and expand the Hadley cell, although weakening and reducing the Polar cell. The Medieval Warm period (A.D. 950–1200) may be an example of that phenomena. Tree-ring data from southern Nevada indicate the region experienced drought during the Medieval Warm period (Graybill and others, 1994).

The arid to semiarid nature of present-day Yucca Mountain climate reflects both its location east of the Sierra Nevada Mountains and its location in the southern edge of the Ferrel cell. During the winter, the

input to the Northern and Southern Hemispheres is seasonally symmetrical, that is, the Northern Hemisphere receives the same amount of heat in its seasons (for example, winter, December) as does the Southern Hemisphere in its equivalent season (for example, winter, June). When the orbit is elliptical, heat input to the tropics varies seasonally, and the heat input to the Northern and Southern Hemispheres is asymmetrical. The change from circular to elliptical orbits occurs over an approximately 100,000-yr (100-ky), but successive cycles differ in magnitude, with four cycles forming a 400-ky cycle (fig. 4).

Obliquity is a measure of the Earth's tilt on its axis (fig. 4). The tilt of the Earth's axis changes from about 22 to 24.5° over approximately a 44-ky cycle. A change in the Earth's axial tilt results in a change in the areal extent of the polar circle and, hence, the relative amount of heat received by the polar region during the year. Obliquity serves to increase or decrease the polar heat deficit relative to the tropics and, in this way, increases or decreases the strength of the Polar cell. The obliquity effect will be expanded or contracted as its periodicity moves in and out of phase with eccentricity.

Precession is a measure of the wobble of the Earth's tilt-axis during the Earth's orbit around the Sun (fig. 4). Today, the Earth's orbit is slightly elliptical, and the Earth is at its minimum distance from the Sun during the Northern Hemisphere winter but is tilted away from the Sun. Necessarily, the Southern Hemisphere is tilted towards the Sun when the Earth is at its minimum distance from the Sun. Thus, the Southern Hemisphere receives more insolation during its summer than does the Northern Hemisphere's summer, and the opposite would be true for the winters. However, because the Earth wobbles on its axis over a 12-ky period, the seasonal minimum and maximum distances to the Sun reverse for the Northern and Southern Hemispheres. So a full precession cycle is 24 ky and is of major importance to the global heat budget. Eccentricity exercises a major influence over precession (fig. 4).

The orbital parameters eccentricity, obliquity, and precession operate on a millennial scale and variously add or subtract to insolation. Insolation at the Equator and in the Northern and Southern Hemispheres correlates with change in the climate system, as described in the section on modern climate. Change in insolation shows a positive correlation with climate change on a global scale. Climate change from glacial to interglacial modes has occurred throughout the last 2 million years (My), with the glacial modes existing about 80 percent of the time. During glacial climate modes, the Polar cell was much larger and supported a continental ice sheet in the Northern Hemisphere. The Ferrel cell was contracted and compressed between the Polar and Hadley cells, and probably the Hadley cell was weaker and reduced in size, lessening its influence over the Earth's heat budget.

Because insolation is calculated from known principles of celestial mechanics, future values of insolation may be determined (fig. 4). The Earth presently falls within the eccentricity 400-ky cycle where, during the next 100-ky subcycle, Earth orbit will describe a relatively circular rather than elliptical orbit. The last time that occurred was 400 ky ago and, as shown in figure 4, insolation for the next 100 ky will be quite similar to that between 400 and 300 ka.

Glacial climate in the Yucca Mountain region was and will be significantly different than the present climate. During a glacial period, the polar front would reside in Nevada year-round and would frequently move south of Yucca Mountain. Therefore, westerly flow with its maritime polar air could occur throughout the year and might dominate the summers, whereas continental polar and arctic air incursions also could occur throughout the year and might dominate the winters. Modern summer circulation patterns with flow from the south likely would not exist during glacial periods due in part to the weakened or fragmented character of the Hadley cell. Glacial climates bring a circulation mode more like that of southern Canada into the southern Nevada region, although due to the Sierra Nevada Mountains and probably to lower specific humidity as a consequence of cooler oceans, precipitation patterns would likely differ from those in Canada.

This somewhat hypothetical discussion of climate change correlated with change in insolation can be shown to apply to the Yucca Mountain region based on the results of studies of long climate records. Such records provide information about how lakes have changed with time and how those changes, when dated, can be compared with insolation curves to establish a correlation. Similarly, the well-dated Devils Hole record of stable isotope changes within the regional carbonate aquifer during the last 500 ky provides a key linkage of regional climate to insolation.

Long Climate Records

Devils Hole

The walls of Devils Hole, a saturated open fracture in the regional Paleozoic-aquifer discharge area 90 km south of Yucca Mountain, are lined with calcite precipitated from the water. Winograd and others (1992) took a 36-cm core from the vein calcite, acquiring an isotopic record of climate change extending from beyond 500 ka to about 60 ka. A chromarine isotopic record of glaciation, whereas high

sand years between actual dates and those from the assumption of orbital timing should not be surprising and although important for eventually understanding the causation of major climate change are not a problem for the issues here. In the case of the Devils Hole record, the glacial intervals appear in step with an orbital clock and disappear in or out of step depending on the particular glaciation.

Owens Lake

The Owens River system (fig. 1), with its sequence of downstream basins (Owens, China, Searles, Panamint, and Death Valley), forms a comparatively simple network where the upstream lakes must spill before the lakes lower in the chain receive sufficient water to freshen (Smith, 1976). The U.S. Geological Survey Global Change and Climate History Program took three cores from the south-central part of Owens Lake playa, Inyo County, Cali-

---

[1]Stable isotopic compositions are typically reported in delta (δ) notation as the per mil deviation of the ratio of the heavy to light isotopes (deuterium to hydrogen, $^{18}O/^{16}O$, $^{13}C/^{12}C$) in the sample to that of a reporting standard. The relation is defined as follows:

$$\delta \text{ (per mil)} = [(R_{sample} - R_{standard})/R_{standard}] \times 1000$$

A similar relation can be used with radiogenic $^{87}Sr/^{86}Sr$ values. Internationally accepted reference standards are Standard Mean Ocean Water (SMOW) as analyzed by the International Atomic Energy Agency (IAEA) in Vienna (VSMOW) for D/H and $^{18}O/^{16}O$, belemnite shell carbonate from the Pee Dee Formation of North Carolina (VPDB) as determined by IAEA for $^{13}C/^{12}C$, and dissolved strontium in modern sea water for $^{87}Sr/^{86}Sr$. By definition, the references standards have $\delta = 0$ per mil. Heavy-isotope enriched or depleted materials have positive or negative δ values, respectively.

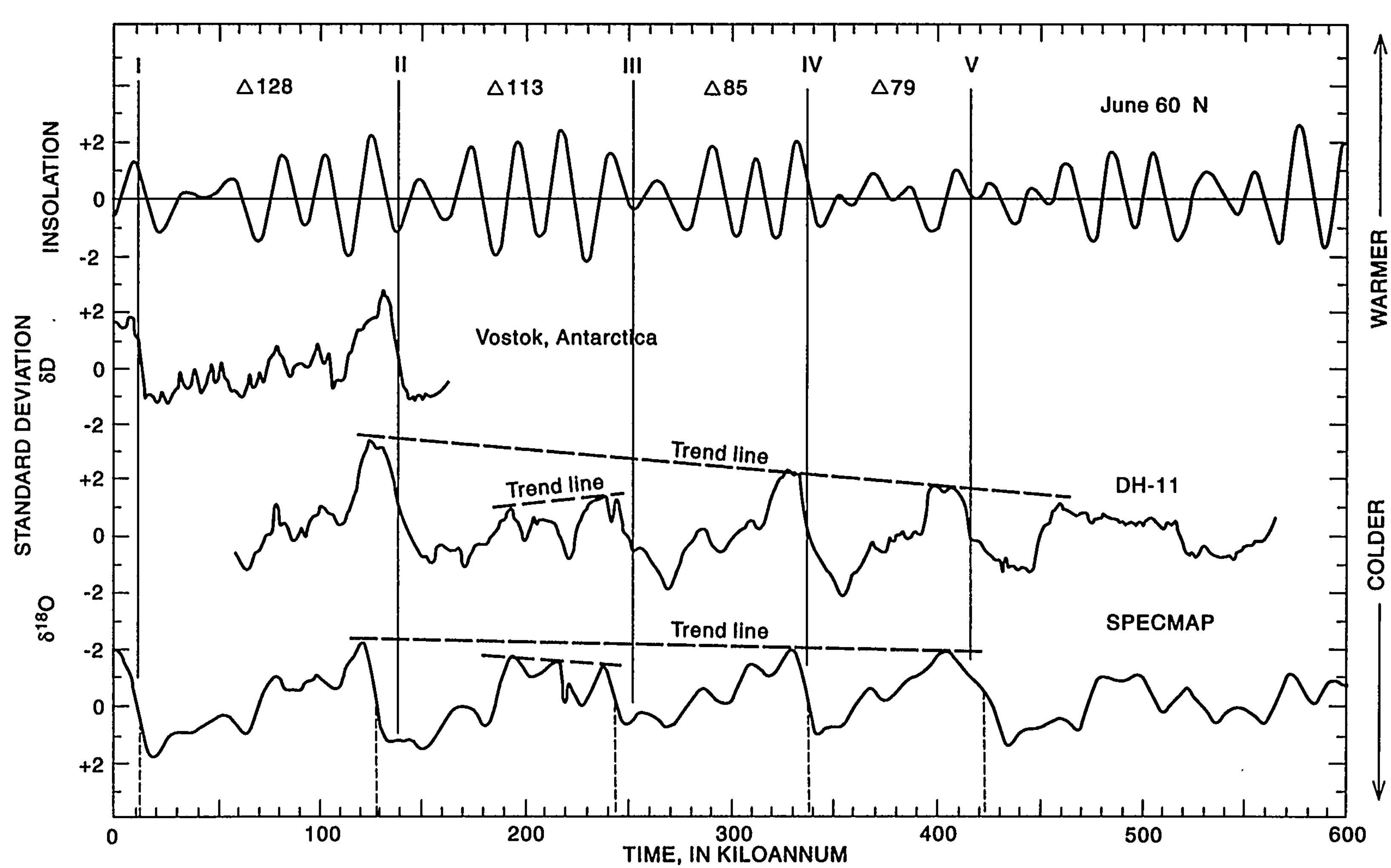

EXPLANATION

Δ128 Time between terminations, in kiloannum

IV Terminations (Broecker and Van Donk, 1970)

| Solid lines represent terminations (approximate midpoints of deglaciations) in DH-11 and Vostok, Antarctica curves

¦ Dashed vertical lines are terminations in the SPECMAP record

Figure 5. Comparison of the delta oxygen-18 record from Devils Hole to other climate records (SPECMAP and Vostok), as well as with the insolation plotted against a time axis. See text and Winograd and others (1992) for discussion.

maintain a perennial, if saline, lake about 6 m deep. The construction of the Los Angeles Aqueduct in 1913 diverted the lake's principal source of water, and the lake soon desiccated in a climate with an evaporation rate of about 1.65 m/yr (Smith, 1976). Locally, alka-

high TDS, and often at elevated temperatures. These waters are derived from the interaction of basin ground waters with reactive fine grained volcanic rocks. Although the primary sources of water for the Owens River apparently come from high elevation, the solute [illegible] climates with reduced mountain flow and greater relative importance of low-elevation spring discharge into Owens Lake. This contrast will be referred to herein as the Owens Lake climate/hydrology relation.

Although this climate/water chemistry linkage identifies relative climate states, it does not yet allow for direct interpretation of MAP or ranges of MAP. The linkage of water chemistry and microfossils to values of MAP is being developed with simple models based on present relations between MAP, water and solute flux, and on relations of microfossils from the last glacial cycle to MAP by means of woodrat midden data from the basin.

Core Stratigraphy

Lithostratigraphy

The upper 225 m of core OL–92 consists predominantly of lacustrine silt and clay interspersed with several thin beds of sand. Some silty units contain up to 40 percent by weight calcium carbonate that reflects large abundance of ostracodes, calcareous algae, and/or authigenic calcite. Much of the silt-sized fraction represents the shells of diatoms and angular

[illegible] rates is believed to be reasonably, but not perfectly accurate. As discussed below, examination of the diatom and ostracode paleoenvironmental stratigraphic sequence shows a regular sequence of interglacial and glacial events. The ages of those events, based on the age model, variously agree or disagree with the Devils Hole Chronology. We believe disagreement of the age model with the Devils Hole chronology simply reflects error in the Owens Lake age model.

Owens Lake Diatom Record

Diatom Analysis

Methods

Samples for diatom analysis of about 1-cm stratigraphic thickness were removed from the split core with a clean spatula and stored in airtight plastic bags. The sediments were processed for diatoms by hot acid digestion, and the cleaned residue was settled on coverslips and mounted in Hyrax (Bradbury, 1993).

Paleohydrologic History of Owens Lake—The Diatom Record

Abundant, loosely attached diatoms (species of "*Fragilaria*") along with planktic species are common from about 500 to 400 ka. The *Fragilaria*-dominated assemblages indicate that Owens Lake was shallow and characterized variously by open water to a through-flowing marsh during this time. Marsh environments probably indicate climates of intermediate moisture and a shallow basin filled by sediment.

Major episodes of freshwater diatoms occur at 470–430 ka, 400–330 ka, 260–220 ka, 170–120 ka, 70–60 ka, and 50–10 ka (fig. 6). In most cases, these intervals indicating cool, wet climates are separated by intervals rich in saline diatoms or intervals with sediments barren of diatoms, which imply shallow, alkaline water conditions. Thus, the diatoms define the long-term climate/hydrological behavior of the Owens River system. The potential rapidity of climate change is illustrated by prominent spikes of freshwater planktic diatoms such as the one between 72 and 65 ka that interrupts the declining trend of saline benthic diatoms (fig. 6).

Overall, the stratigraphic continuity of freshwater diatoms from Owens Lake indicates a record of a longer-lasting and more persistent fresh and overflowing lake system than that of a shallow, saline system. The concentration of freshwater diatoms, in direct contrast to the ostracodes, is generally an order of magnitude greater than concentrations of saline diatoms, partly reflecting poor diatom preservation in saline systems. Therefore, rare and short-lived episodes of high concentrations of saline planktic diatoms, implying large and possibly deep saline lakes, may be underrepresented in the Owens Lake record and contrast with the paleolimnology of internally draining Great Basin lakes such as Walker Lake (Bradbury and others, 1989).

Over the past 500 ky, Owens Lake has been fresh (implying climates wetter than today) for about 80 percent of the time and saline (implying climates like today) only about 20 percent of the time. Although there is some variation, intervals of wet climate (freshwater conditions) average about 32 ky in length, whereas dry climates (saline conditions) average about 13 ky.

Owens Lake Ostracode Record

Ostracode Methods

The climate interpretations derived from the ostracodes found in the Owens Lake cores are based on 672 samples covering the past 400 ky. About 75 percent of those core samples contained sufficient ostracodes for environmental interpretations. Each sample covers about a 5-cm-thick stratigraphic interval, and a sample was taken every 20 cm in core from the upper 200 ky and every 33 cm from material below 200 ky. The valves were extracted from the sediments and the adults identified and counted. The data set discussed below is based on a total count of 145,000 valves.

Paleolimnological History of Owens Lake—The Ostracode Record

The stratigraphic profile (fig. 7) of the ostracodes found in the Owens Lake record shows how the lake's hydrochemistry has changed during the last 400 ky. The ostracodes are arranged in the diagram according to hydrochemical tolerances. *Limnocythere sappaensis,* on the right side of the graph (fig. 7), lives in the springs that discharge onto the lake floor today, such as those near Keeler on the northeastern side of the lake and at Dirty Socks Spring on the southern side of the lake. Thus, *L. sappaensis* marks modern-like periods when flow from high elevation was minimal and flow plus solute input from low elevation was maximal. *Cytherissa lacustris,* on the left of the graph (fig. 7), represents limnological and climatic periods least like those of today. It implies the presence of a large, deep, seasonally stable, cold, dilute freshwater lake dominated by source waters from high elevations. *Candona caudata* and *Limnocythere c.f. L. friabilis* may live in the same environments as *C.lacustris,* as well as in smaller lakes at higher TDS and temperatures (Bradbury and others, 1989). Presence of *L. c.f. L. friabilis* implies continued dominance by waters from high elevation (Forester and others, 1994) but at times, when *C. lacustris* is absent, with less flow. The taxa in the center of the graph (fig. 7), such as *Limnocythere ceriotuberosa,* identify periods when the lake was supported by a mixture of high- and low-elevation source waters (Forester, 1986). They further indicate the existence of a seasonal lake variable in size, depth, TDS, and temperature. The source water during these

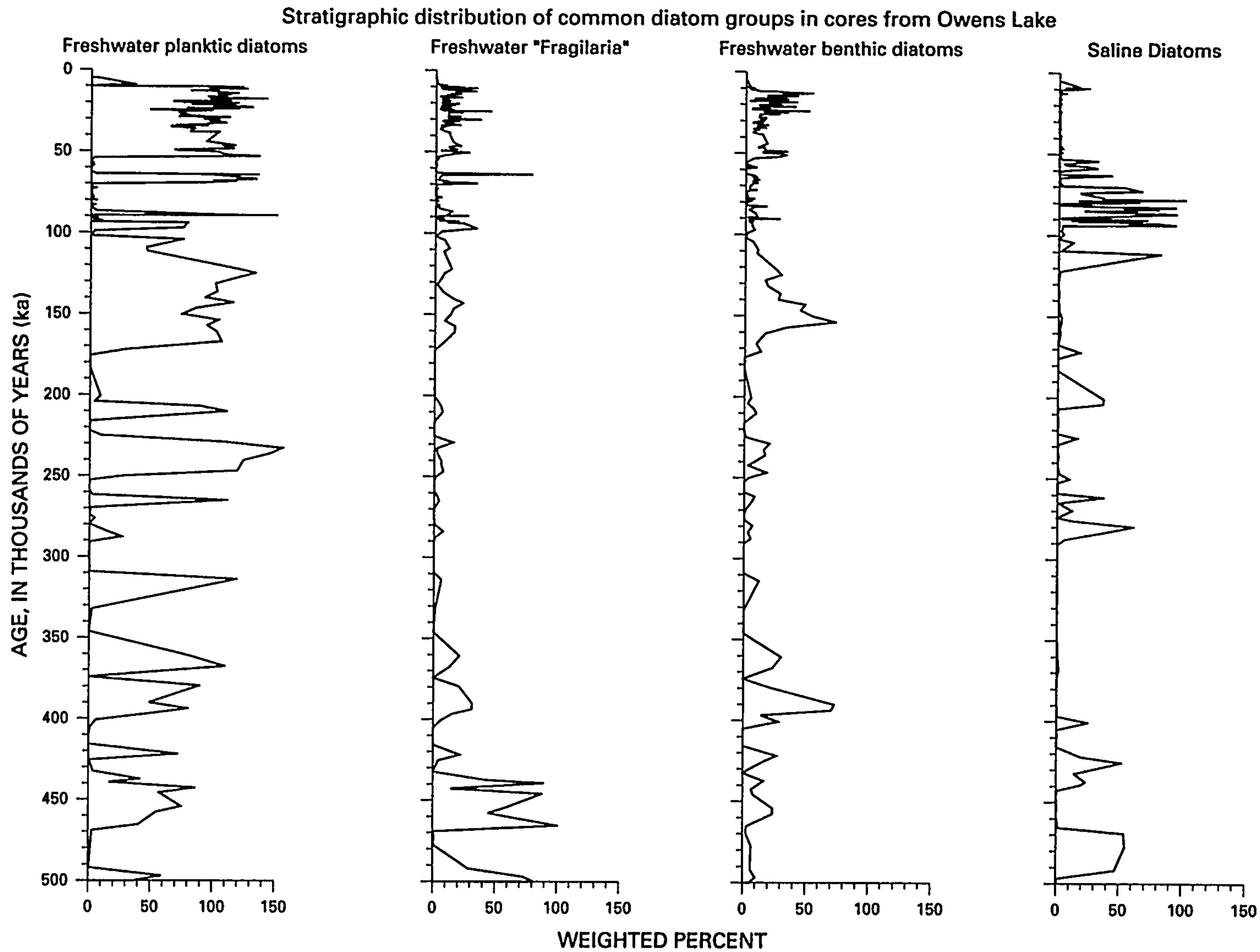

Figure 6. Relative abundance in weight percent of various kinds of diatoms from Owens Lake, California. The saline diatom profile identifies the dry climate, typically interglacial periods. All other periods are wetter than modern day. See text for discussion.

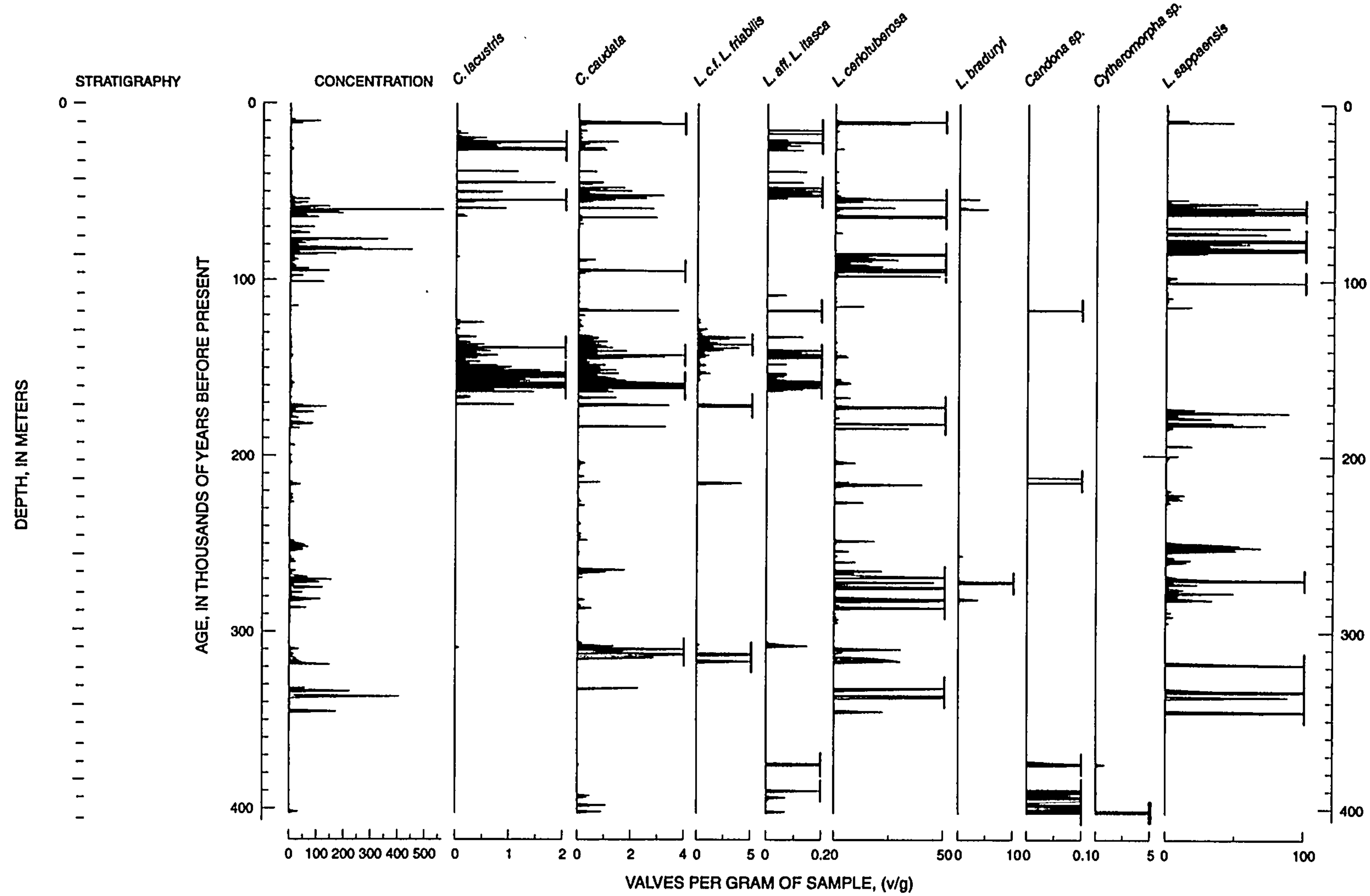

Figure 7. Relative abundance of various ostracode species in valves per gram found in Owens Lake, California, plotted against a generalized lithologic column. The ostracodes are aligned according to their salinity and, hence, climate preferences from fresh, cold, and wet on the left (towards the stratigraphic column) to saline and dry on the right. *L. sappaensis* on the right lives in springs discharging onto the lake bed today.

[illegible]

Cytherissa lacustris represents the extreme cold and/or wet phases in the ostracode record. It occupies about 5 percent of the samples and occurs almost exclusively from about 170 to 130 ka and from about 60 ka sporadically to 18 ka (fig. 7). Similarly, *Candona caudata* and *Limnocythere c.f. L. friabilis* distributions are characteristic of the upper half of the Owens Lake record. The absence of *C. lacustris* in sediments from about 400 ka to 170 ka indicates "warmer" glacial periods than existed during the last two glacial periods. Thus, the ostracode climate/hydrological record of Owens Lake indicates the four 100-ky climate subcycles are not climatically identical to one another.

The ostracode record also shows how rapidly climate changes in this region. Change from modern-like *Limnocythere sappaensis* periods to wetter periods typically occurred in hundreds, not thousands, of years. Such rapid changes from warm/dry to cold/wet climates indicate a southerly shift in the average position and strengthening of the westerly/polar front associated with the polar jet stream.

Correlation of Owens Lake Paleolimnology and Oxygen Isotope Records

The Owens Lake chronology is based entirely on a sediment accumulation rate age model (Bischoff and others, 1993). The age of a particular sample, as derived from the age model, could be older or younger than the actual age of the sample. Because the rate of sediment accumulation may be expected to change in a lake basin, the calculated versus real ages may converge at some depths and diverge at others. However, the derived, extrapolated chronology

[illegible] be tuned to the Devils Hole or SPECMAP records.

A good correlation exists, after considering the above paragraph, between the diatom and ostracode Owens Lake climate/hydrological records, SPECMAP, and the Devils Hole record of global climate change known as Oxygen Isotope Stages (OIS) (figs. 8 and 9). The diatom record (fig. 8), indicating large freshwater lakes, shows prominent intervals at 470–430 ka (OIS 12), 400–310 ka (OIS 10), 250–220 ka (OIS 8 falls between 280 and 250 ka), 170–110[2] ka (OIS 6), 72–65 ka (OIS 4), and generally after 50 ka (OIS 3+2) until the Holocene (<10 ka, OIS 1). The discrepancy between the diatom record and OIS 8 probably indicates a problem with the Owens Lake age model.

The ostracode record (fig. 9) shows a pattern similar to that of the diatoms, but owing to the preservational differences, the ostracode record offers a better indication of the interglacial periods and transitions to glacial periods than of the glacial intervals. The ostracode record from 400 ka shows a transition into OIS 10; then a barren interval; followed by saline conditions from about 350 to 320 ka (OIS 9); then a mix of fresh, intermediate, and saline waters, 300 to 220 ka (OIS 8); then saline conditions from 200 to 180 ka (OIS 7); saline from about 115 to 95 ka (middle of OIS 5); then saline again from 85 to 70 ka (end of OIS 5); saline again from 60 to 50 ka (part of OIS 3); and, finally, saline conditions from 10 to 0 ka (OIS 1). The ostracodes also identify prominent wet periods from 170 to 140 ka (OIS 6) and sporadically from about 55 to 40 ka (part of OIS 3) and from about 25 to 18 ka (OIS 2).

Significantly for this project, the ostracode data imply that the first two glacial periods in the past

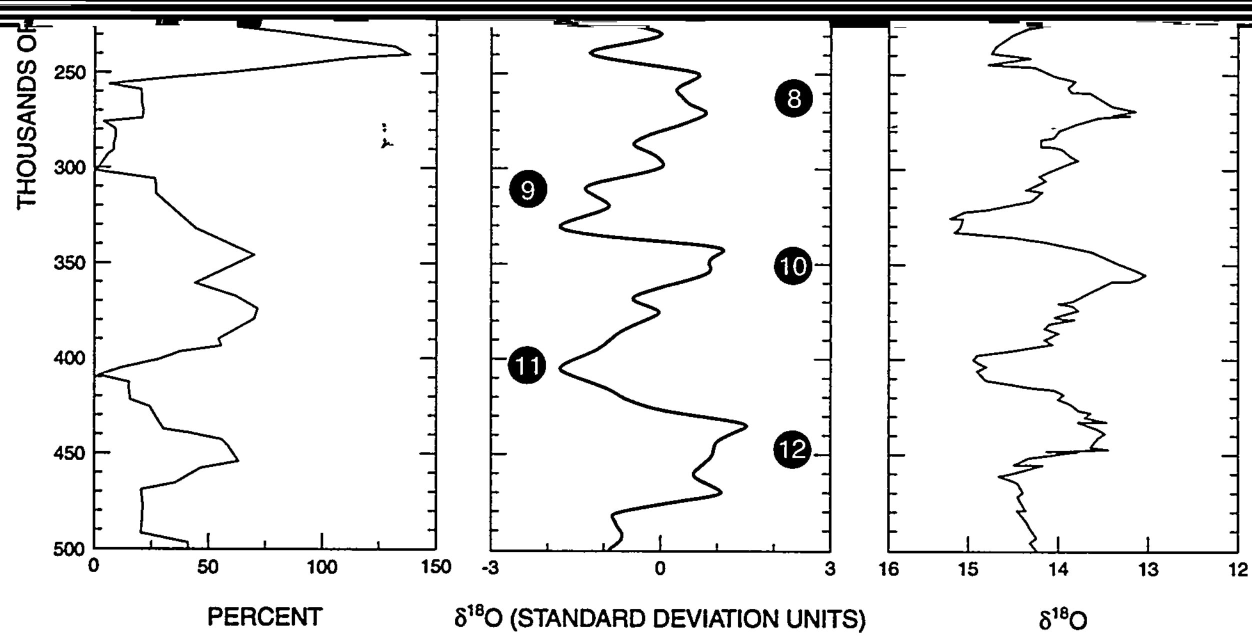

Figure 8. The freshwater planktic diatom stratigraphic distribution from Owens Lake compared to the SPECMAP and Devils Hole records. Even numbers in circles next to SPECMAP profile identify the widely recognized stable isotope glacial periods recognized from oceanographic records, and the odd numbers identify the interglacial periods. Each number refers to a particular oxygen isotope stage (OIS).

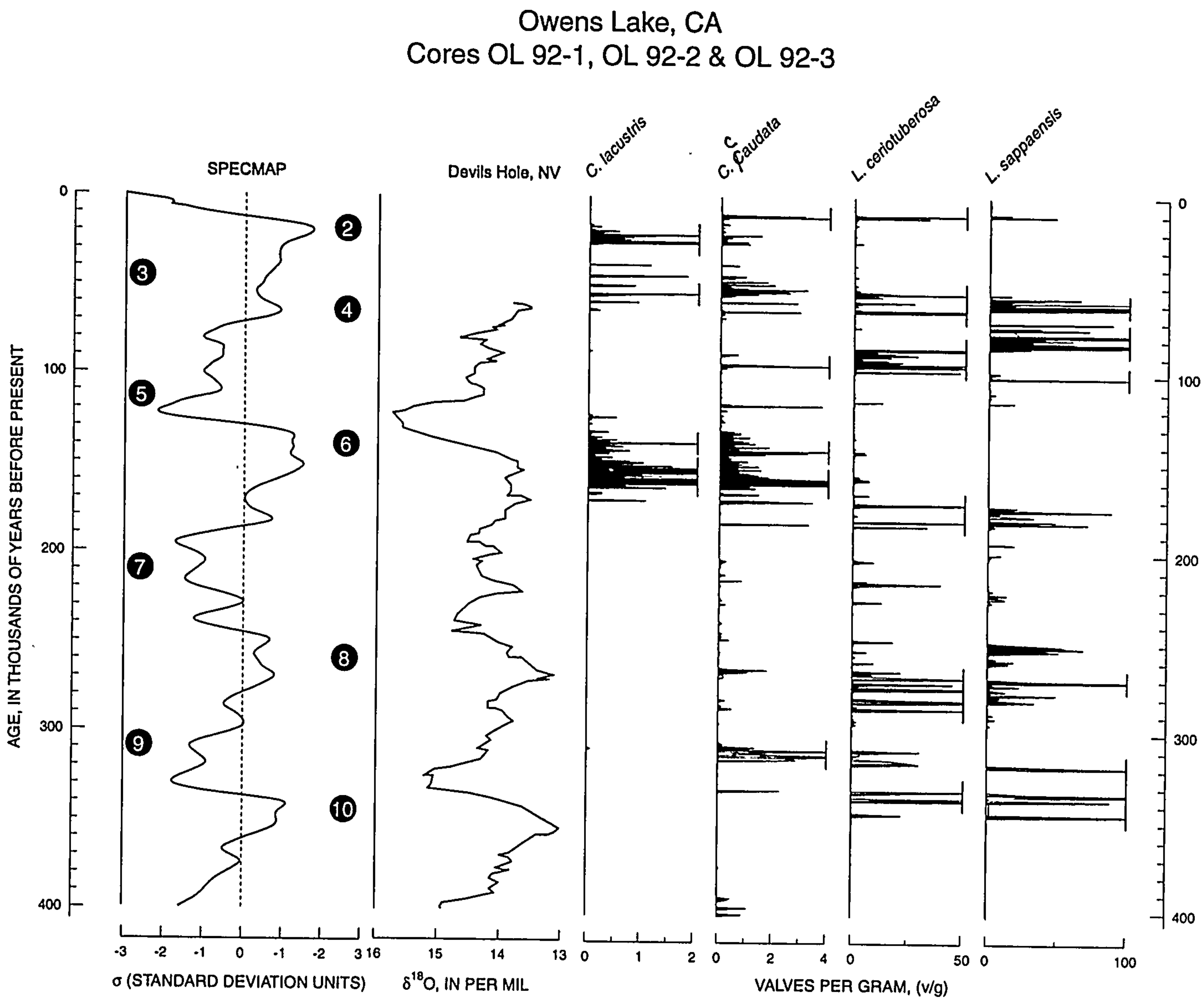

Figure 9. Key ostracode species stratigraphic profiles from Owens Lake compared to the SPECMAP and Devils Hole climate records. Numbers in circles identify the glacial and interglacial oxygen-isotope stages (OIS) for the last 400-ky climate cycle.

through the relative quantities of water and solutes delivered to the lake during different climate modes. The microfossil record from Owens Lake serves as a proxy for the climate/hydrological couplet and shows that, during the past 400 ky, climate was wetter than modern about 80 percent of the time.

2. The wet periods coincide with the long, complex glacial climates. Most of those glacial climate periods correlate with the SPECMAP and Devils Hole records of global climate change and thereby indicate that future climate change may occur on a schedule that is related to the changes in the Earth's astronomically based insolation cycle.
3. The Owens Lake record indicates that climate during the various glacial periods was not

these former wetlands and interpreted the environments associated with them. A variety of fossils, including mammals, molluscs, ostracodes, pollen, impressions of leaves from trees and shrubs, and diatoms have been identified from the paleowetland sediments. Mammal remains range from meadow mice of marsh environments to mammoths, reflecting the diverse terrestrial communities supported by past climates in southern Nevada.

Deposits from the Las Vegas, Indian Springs, and Pahrump Valleys, as well as Crater Flat, Lathrop Wells, and the Amargosa Valley have been studied during Yucca Mountain project site characterization activities and collected for fossils. The sites along the Yucca Mountain ground-water flow gradient are discussed in the section on past discharge and will not be treated in this section.

Sites from the Pahrump Valley, such as the Hidden Valley or the Stump Spring sections, contain paleoclimatic and paleohydrological information, but past aquatic environments at those sites also may reflect fault control of the hydrology (Quade and others, 1995) so the water table does not rise uniformly along the valley bottom. Discussion of those sites awaits the distinction of the climate/hydrological signal from tectonic overprints, which could affect flow properties and, hence, the climate signal. The records from the Las Vegas and Indian Springs Valleys contain good climate and hydrological information based on sediment stratigraphy and fossils. Fossil data from one of those sections, OCI–11, are discussed below, as its environmental information is representative of the other sections.

Corn Creek Flat (Main) Section OCI–11

Section OCI–11 (fig. 10) lies near the center of the Las Vegas Valley (figs. 1, 2D). The informal stratigraphic units denoted B, D, and E were described by Quade (1986). These units are distinguished from each other by a variety of sedimentary features such as bed forms, grain size, color, rhizolith (rhizolith = rootstone = carbonate or opal cemented sediment coatings formed when root decomposes?) content, and fossils (Quade, 1986; Quade and Pratt, 1989; Quade and others, 1995). Units B and D occur throughout the Las Vegas Valley, indicating extensive wetlands.

Twenty-two radiocarbon dates constrain the age of these sediments. Radiocarbon dates from unit B imply it is older than the limit of radiocarbon detection, about 40 ky. The unit B ostracode assemblage indicates a cool and wet climate, perhaps correlating to the penultimate glacial period (170 to 140 ka) or the early part of the middle Wisconsin interval (70 to 60 ka; see, for example, the Owens Lake climate record). Conversely, unit D radiocarbon dates show it was deposited during the last glacial cycle. Similarly, dates on unit E indicate deposition at the end of the last glacial cycle during the climate transition to the Holocene.

The abundant ostracodes (fig. 10) and molluscs in unit B indicate this environment was a shallow, relatively freshwater, typically permanent wetland supported by the regional water table and flowing springs. Climate parameters, as yet, have not been generated from the ostracodes in unit B. Nonetheless, the persistence of a fresh, permanent wetland on the Las Vegas Valley floor where modern effective moisture deficits are more than 1,000 mm requires a substantial shift in some combination of increased MAP and decreased MAT.

The ostracode taxa from unit D also indicate a wetland spring complex similar to the assemblages from unit B (fig. 10). Unit D species imply this wetland had a higher flow component than did unit B. Further, the smaller quantity of aquifer species in unit D may indicate less discharge from the regional aquifer. Forester and Smith (1994) estimated MAP based on ostracodes from a nearby section (LPM-34, fig. 2D). They indicated MAP was four to five times higher than today. However, they did not recognize the importance of flow through the wetlands. The existence of flow creates an illusion of higher MAP, because flowing water is usually less thermally and evaporatively coupled to the atmosphere than standing water. The MAP levels of 400 to 600 mm reported by Forester and Smith (1994) probably did exist in this area but only at higher elevation where present MAP is also higher. Thus, the change in MAP between today and the last glacial interval on the valley floor, where MAP is 112 mm, was probably less than about four times modern.

The ostracode assemblages found in unit D commonly live in eastern Washington and western Minnesota today where MAT is 5 to 7°C, and effective moisture deficits are about 200 mm or roughly five times lower than that of the modern-day Las Vegas Valley (Forester and Smith, 1994). The MAT values (like MAP) may be too cold for valley bottoms but, considering factors such as cold air drainage, they may be closer to actual paleovalues than is MAP. Reduced MAT in the Las Vegas Valley must have contributed significantly to changes in past levels of effective moisture, along with a probable double increase in MAP.

The ostracodes found in unit E contain more spring species and fewer wetland and aquifer species. Because section OCI–11 is from the valley floor, large wetlands, if they existed, would have covered this site, so the absence of wetland taxa implies fewer or smaller wetlands, which indicates lower effective moisture relative to the glacial intervals.

The radiocarbon ages document the timing of the growth and decline of the unit D and E wetlands. The wetlands existed around 36 ka, and they persisted until 12.1 ka at section OCI–11 (fig. 10) and to somewhat younger times in nearby sections. The growth and persistence of wetlands in southern Nevada is

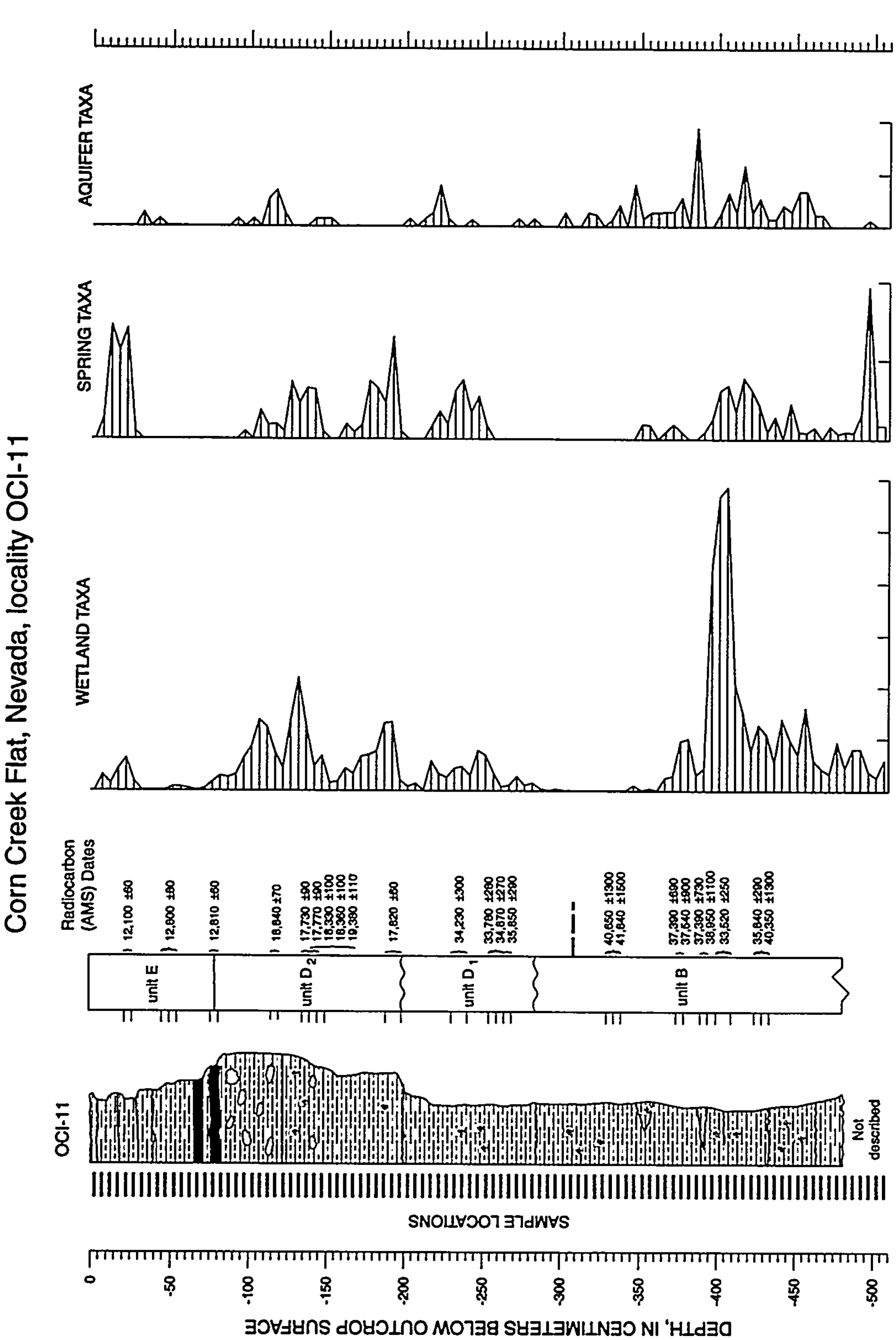

Figure 10. The stratigraphic distribution of key kinds of ostracodes compared to their stratigraphic record. Radiocarbon ages, derived largely from mollusc shells, are shown versus the unit stratigraphy identified and described by Quade (1986). See text for discussion.

Basin Desert to the north (Hunt, 1973) (fig. 1, 11). The climate and vegetation in the region are influenced by three climatic systems (Houghton, 1969; Houghton and others, 1975):

Pacific: A regime dominated by maritime polar air masses created when the edge of the Polar cell moves south in winter. These cool, moist air masses from the Pacific Ocean produce cool, wet winters and hot, dry summers. Plant species favoring this regime extend into southern Nevada from west and northwest of Yucca Mountain.

Gulf: A regime dominated by maritime and continental tropical air masses resulting from

pine elements, indicating links to the Rocky Mountains and moderate connections to the Sierra Nevada (Cronquist and others, 1972; Charlet, 1995).

Results and Discussion

The presence or absence of limber pine (*Pinus flexilis*) and white fir (*Abies concolor*) in the late Pleistocene woodrat-midden record identifies cooler-drier or warmer-wetter climate regimes. During certain periods, these trees grew at elevations much lower than today. Modern elevational and geographic distributions are used to infer past climatic conditions.

Table 1. Modern vegetation distributions within the Yucca Mountain area. Habitats of various species are shown.

[m, meters; ft, feet (both indicating elevations)]

Habitat	Sarcobatus	Sphaeralcea	Ambrosia	Atriplex confertifolia	Enogonum	Opuntia	Atriplex	Stipa hymenoides	Ceratoides lanata	Ambrosia dumosa	Lycium andersonii	Larrea tridentata	Distichlis	Grayia spinosa	Ephedra	Tetradymia	Salizaria mexicana	Yucca schidigera	Artemisia	Yucca brevifolia	Coleogyne ramosissima	Haplopappus	Chrysothamnus	Fallugia paradoxa	Yucca bacata	Artemesia tridentata	Cercocarpus	Juniperus osteosperma	Pinus monophylla	Cowania	Prunus fasciculata	Quercus gambelii	Acer	Juniperus communis	Populus tremuloides	Abies concolor	Pinus flexilis	Pinus ponderosa	Pinus longaeva	Populus fremontii	Salix	Prosopis	Fraxinus
Spring/seepage areas			X	X	X	X	X			X	X	X	X		X							X	X									X								X	X	X	X
Arroyos		X	X		X		X										X					X	X	X							X	X									X		
Upper elevations 2,750–3,505 m (9,020–11,500 ft)																																				X	X	X	X				
2,195–2,750 m (7,200–9,020 ft)									X							X			X	X						X	X	X	X			X	X	X	X	X	X	X					
1,830–2,195 m (6,000–7,200 ft)							X	X	X				X	X	X	X			X	X			X	X	X	X	X	X	X	X	X	X											
Lower slopes 1,220–1,830 m (4,000–6,000 ft)				X	X	X	X	X	X			X	X	X	X	X	X	X	X	X	X	X	X	X	X	X	X	X	X														
Upper Bajadas 1,065–1,220m (3,500–4,000 ft)			X	X	X	X	X	X	X	X	X	X	X	X	X	X	X	X	X	X																							
Lower Bajadas 150–1,065 m (500–3,500 ft)		X	X	X	X	X	X	X	X	X	X	X	X	X	X	X																											
Basin floor	X	X	X	X	X	X	X	X	X																																		

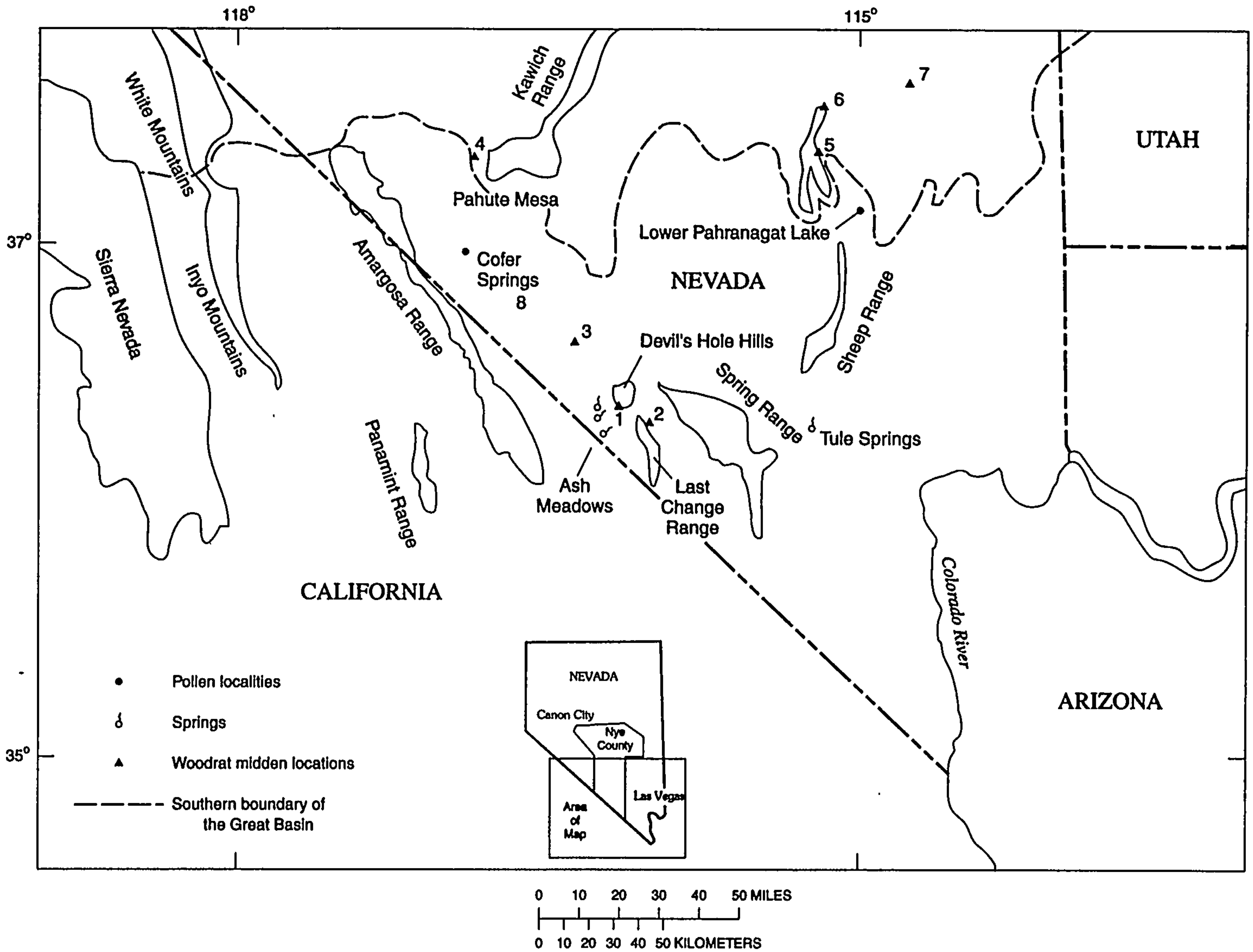

Figure 11. Southern Nevada woodrat-midden localities mentioned in this study. These include (1) Owl Canyon, (2) Last Chance Range, (3) Little Skull Mountain, (4) Ribbon Cliffs, (5) Pahranagat Range-southeast of Badger Mountain, (6) Pahranagat Range-Hancock Summit, (7) Pahroc Springs, and (8) Yucca Mountain.

Limber Pine

The current habitat of limber pine is characterized by dry, continental climate with wide annual and diurnal temperature fluctuations. The mean annual precipitation (MAP) ranges from 380 to 560 mm and is distributed evenly throughout the year (Steele, 1990). Limber pine is common between 1,981- and 2,743-m elevation, primarily in the Rocky Mountains. It presently grows between 2,195- and 3,505-m elevation on the Nevada Test Site (Beatley, 1976).

White Fir

The taxonomy of white fir recently has been amended to split the population into the Sierra white fir (*Abies lowiana*) and Rocky Mountain white fir (*Abies concolor*) by the Flora of North America Editorial Committee (1993); most descriptions of western North American plants still join the two species as *Abies concolor.* No attempt yet has been made to differentiate the species in our midden material, although this may be possible in the future.

Sierra white fir grows in areas dominated by the moist Pacific climate regime with MAP ranges from 890 to 1,240 cm. Rocky Mountain white fir grows on high mountains dominated by drier continental climate with MAP ranges from 510 mm to greater than 890 mm. White fir is common between 1,200- and 2,100-m elevation (Laacke, 1990). Isolated colonies of white fir grow in the Spring Mountains and on Bald Mountain in the Groom Range of Nevada (U.S. Air Force, 1986). Currently, the colonies are associated with the Rocky Mountain taxon, but, during the Pleistocene, either or both of the white fir species could have inhabited southern Nevada.

Fossil Record

Spatial and Chronological Continuity of Data

The woodrat-midden data base can be affected by (1) environmental limits that constrain the geographical distribution of woodrats, and (2) wetter climates that could destroy woodrat middens after formation. Today, two woodrat species elevationally overlap from valley floors (desert woodrat, *Neotoma lepida*) to the mountain tops (bushy-tailed woodrat, *N. cinerea*), occupying all but the most extreme habitats in the Great Basin (Hall, 1995). The current range of the bushy-tailed woodrat, which seems to have been the dominant species in the Great Basin during the late Pleistocene, includes the southern Yukon where the climate is substantially wetter and colder than that of the modern Great Basin. Woodrat middens of varying ages are found throughout the elevational and geographic ranges of these two species.

Widely divergent radiocarbon dates on materials obtained from single woodrat midden strata for the late Quaternary indicate that midden resolution and destruction was accelerated prior to 14 ka (Spaulding, 1985, 1990; Van Devender and others, 1986). Although only 23 percent of the dated woodrat midden strata in the Yucca Mountain area are older than this date, climate regimes are adequately represented.

Timing

Limber pine appears regularly in the record between approximately 13 to 11 ka, 21 to 14 ka, 26.5 to 23 ka, and 33 to 29 ka (fig. 12). Four periods of white fir occurrence at elevations lower than today center around 13 to 12 ka, 16 to 14 ka, 26 to 21 ka, and about 35 to 32 ka (fig. 13). Periods when climate appears to exclude white fir from communities with abundant limber pine occur from 21 to 16 and 32 to 29 ka. Periods when climate appears to include white fir without major limber pine association are from 23 to 21 and 35 to 33 ka.

Elevational Displacement

The lower elevation of middens containing limber pine and/or white fir macrofossils coincides with the base of modern semiarid pinyon-juniper woodland, about 1,220 m. The displacement of limber pine and white fir to lower elevations by as much as 1,000 m during the Pleistocene records significant real increases in MAP that cannot be explained simply through reduced MAT. Corroborating data indicate limber pine was growing between 1,500 and 1,300 m in the Eleana, Sheep, and Spring Ranges, Fortymile Canyon, and Clark Mountain during the Pleistocene (W.G. Spaulding, 1981, 1985, 1990; Dames and Moore, written commun., 1994; Mead and others, 1978; Mehringer and Ferguson, 1969).

Environmental Parameters

Although limber pine and white fir grow together today in some places, white fir typically requires warmer winter temperatures and more annual

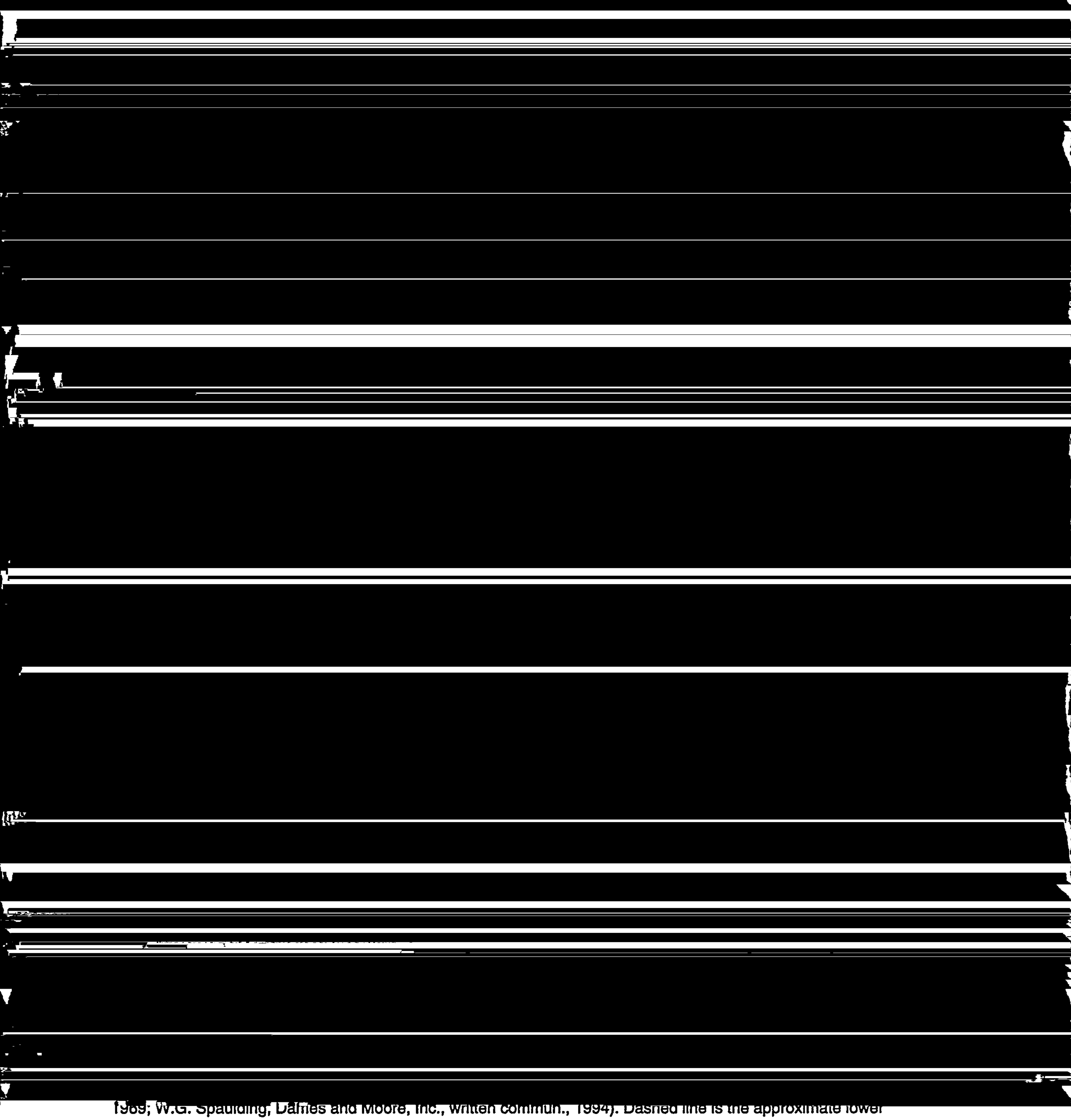

1989; W.G. Spaulding, Dames and Moore, Inc., written commun., 1994). Dashed line is the approximate lower elevational distribution limit of limber pine in the Sheep Range today. Middle, radiocarbon dates on limber pine from Spaulding (1985) plotted as a normal distribution at three standard deviations around the mean. Bottom, radiocarbon dates on limber pine for other studies plotted as a normal distribution at three standard deviations around the mean. For the middle and bottom plots, the normal distributions are a measure of radiocarbon date precision, that is, the more pointed the distribution curve, the more precise the date, and the flatter the curve, the less precise the radiocarbon date.

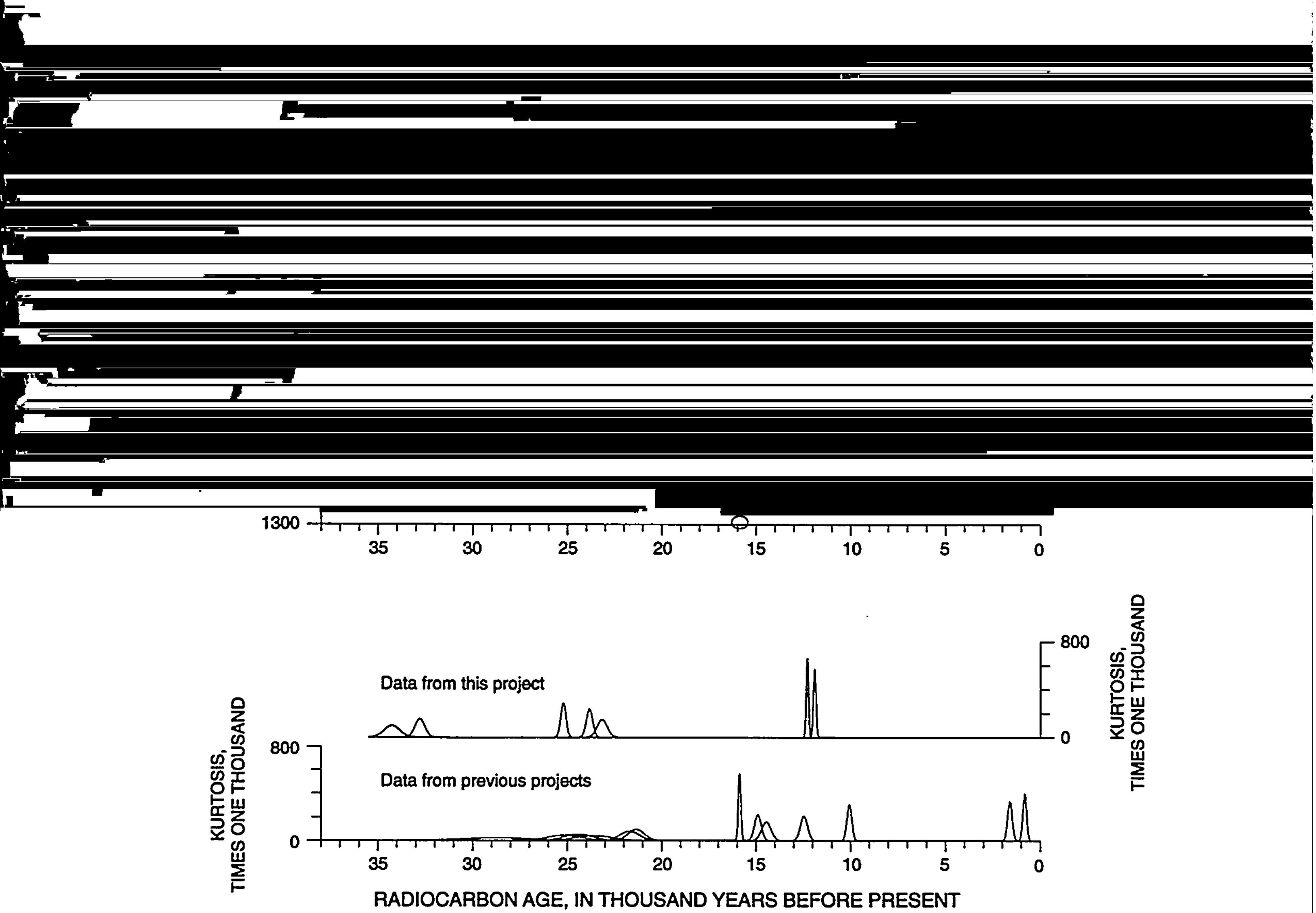

Figure 13. Age plotted against elevation for white fir in the Yucca Mountain area, Nevada. Top, chronologic plot of the elevational distribution of directly dated white fir macrofossils from ancient woodrat middens from a 200-km radius around Yucca Mountain (our own data and Spaulding, 1981; Mead and others, 1978; Mehringer and Ferguson, 1969; dashed line is the approximate lower elevational distribution limit of white fir in the Sheep Range today); middle, radiocarbon dates on white fir for this study plotted as a normal distribution at three standard deviations around the mean; and bottom, radiocarbon dates on white fir from Spaulding (1985) plotted as a normal distribution at three standard deviations around the mean. For the middle and bottom plots, the normal distributions are a measure of radiocarbon date precision, that is, the more pointed the distribution curve, the more precise the date, and the flatter the curve, the less precise the radiocarbon date.

Pleistocene (Wells and Jorgensen, 1964; Wells and Berger, 1967; W.G. Spaulding, 1977, 1981, 1985, 1990, Dames and Moore, written commun., 1994; Mehringer and Warren, 1976; Wells and Woodcock, 1985). At upper elevations, it commonly occurred in association with limber pine and in some cases with white fir (Mehringer and Ferguson, 1969; Spaulding, 1977, 1981, 1985, 1990). Due to woodrat collection bias, juniper is common to abundant in most late Pleistocene woodrat-midden strata; this does not mean that it was consistently the most abundant species at all elevations. Both woodrat-midden and pollen evidence indicate that the bulk of Utah juniper's Pleistocene distribution lay at lower elevations and not at upper elevations (Mehringer, 1967; Wells and Woodcock, 1985).

Today, the MAP of Utah juniper ranges between 410 to 250 mm (U.S. Forest Service SCS DATA BANK; U.S. Air Force, 1986). The lower MAP value of limber pine overlaps with the upper MAP value of juniper. This indicates a minimum MAP of 380 to 410 mm where the two species occur together in the fossil record. The minimum MAP of Rocky Mountain white fir is higher: 510 mm. This would indicate a MAP above 410 mm or increased winter soil moisture during the time periods containing all three species.

achieved through the examination of associated shrubs, forbs, and grasses. A total of 56 taxa were identified, and 18 of these were determined to be the best climatic indicators (table 2).

In general, the more mesic (wetter) shrubs (for example, sagebrush, *Artemisia spp.*) found in association with limber pine and white fir during the Pleistocene have upper MAP ranges around 400 to 420 mm. More xeric (drier) shrubs (for example, shadscale, *Atriplex spp.*, and winterfat, *Ceratoides sp.*) have upper MAP ranges around 150 to 250 mm U.S. Forest Service SCS DATA BANK). These data indicate that effective moisture during periods of wetter climate should be constrained toward the more

end of the MAP scale of limber pine during periods when white fir occurred. Thus, if the lower MAP range of the modern juniper community is compared with the lower MAP values of limber pine, a MAP 1.9 times the present MAP (an increase from a MAP value of 200 to 380 mm) can be derived. (Ongoing refinement of MAP values may change the final percentage of increase.) This increase allowed limber pine to migrate through the current elevational distribution of Utah juniper to at least the current lower boundary of juniper. At lower elevations, the movement of Utah juniper into areas currently occupied by shadscale would require MAP 1.3 times the present (a shift from 150 to 200 mm).

Table 2. Plant contents of radiocarbon-dated middens at key localities around southern [redacted]

[Ages are ^{14}carbon ages, reported in "years before the present"; m, meters]

	OC210594ARM8	OC020469PJM1(2)	OC210594MLH7(5) can frt	OC210594MLH7(1)C	OC210594MLH7(1)B	OC210594MLH7(1)A	OC150589PEW2(1)	OC020469PJM1(1)	OC020469PJM1(3)	OC150589PEW1(1) unit on ceiling, bottom unit	OC150589PEW1(1) above middle layer	LSM151182LP1(2,2)	LSM151182LP1(2,1)	LSM151182LP1(2,3)	LSM151182LP1(2,4)	LSM151182LP1(3,1)	LSM151182LP1(3,2)	LSM151182LP1(4)	LSM151182LP1(1)	LSM141282RR1(1)	LSM120882LP1(1)	PR240584PEW1 [redacted]	PR100588P [redacted]	PR240 [redacted]	P [redacted]
Elevation, m	800	800	800	800	800	800	800	800	800	800	800	1,200	1,200	1,200	1,200	1,200	1,200	1,200	1,200	1,200	1,200	**	1,600	**	**
Age ^{14}C yr B.P.	37,900	21,500	20,000	18,900	18,600	13,500	12,300	9,500	8,200	4,000	1,700	14,300	13,700	12,000	10,500	10,000	9,500	8,500	6,700	2,000	1,100	33,300	22,700	21,400	13,500
Abies concolor																									
Pinus flexilis																							#		
Celtis reticulata																		#							
Pinus monophylla									#																
Purshia tridentata										#				#	#										
Symphoricarpos longiflorus	#			#	#	#		#	#																
Artemisia tridentata																						#			
Juniperus osteosperma	#	#	#	#	#	#	#	#	#			#	#	#	#		#					#	#	#	#
Prunus fasciculata								#	#																
Salvia dorrii			#					#	#	#	#		#		#		#								
Stipa hymenoides		#	#					#				#	#	#	#		#				#	#			#
Tetradymia glabrata		#	#				#		#																#
Yucca brevifolia													#												
Ephedra								#	#	#	#		#		#	#	#		#			#	#		
Atriplex canescens																									
Cactaceae		#						#	#	#	#	#	#		#		#						#	#	#
Larrea tridentata								#	#	#	#								#		#			#	
Atriplex confertifolia	#	#	#	#	#	#	#	#				#			#	#			#	#	#	#			

[redacted]

Nevada. Radiocarbon date distributions currently available from woodrat midden macrofossils indicate that the durations of these periods appear to be relatively short, less than 1500 years, and that onset and

elevations of 1,500 m than it was at 750 m. Lack of data above 2,000 m for the Pleistocene prevents extrapolation of precipitation increases to higher elevations using plant remains from woodrat middens.

[redacted]

The Fluvial Record of Fortymile Wash

Fortymile Wash, an ephemeral desert-wash tributary to the Amargosa River, is the major surface-water drainage on the eastern side of Yucca Mountain and for a much larger area of uplands to the northeast (fig. 1). The alluvial history of Fortymile Wash has been constrained by thermoluminescence (TL) and ^{230}Th/U dating of the surficial and buried soils.

The relations between the alluvial materials, the soils, and their ages together with other local climate records indicate the following preliminary hypothesis: Fortymile Wash aggrades during interglacial and transitional climates that produce high-intensity rainfall and runoff. These intense rainfall and runoff events erode hillslopes, including those of Yucca Mountain, and thereby supply abundant sediment to the fluvial system. Fanhead incision on Fortymile Wash occurs during relatively cool and moist climates when hillslopes are relatively stable and supply little sediment to the flows of Fortymile Wash, which were perhaps sustained by concentrated spring snowmelt from its upper basin. The discussion below describes the ages and relations of the surficial deposits that were used to support this hypothesis.

The Quaternary history of lower Fortymile Wash is characterized by the aggradation of a large alluvial fan extending into the central Amargosa Desert with some incision in the upper part of the fan. Although significant aggradation has occurred on the lower central part of this fan during the Holocene, a larger episode of aggradation occurred during the Pleistocene between about 120 and 50 ka, resulting in deposition of the uppermost layer of coarse gravel that forms the present high terrace surface near Yucca Mountain.

Incision of the uppermost part of the Fortymile Wash fan occurred before the last glacial maximum. This is indicated by the minimum ages of secondary U-rich opal/carbonate coats on clasts, and by the presence of a silty argillic horizon in the surface soil (Lundstrom, Westling, and others, in press; Lundstrom, Mahan, and Paces, in press; Lundstrom, Whitney, and others, in press). Fanhead incision reaches a maximum of about 25 m near well J–13 and at the latitude of the potential repository.

Younger inset alluvial units that occur along the incised upper part of the Fortymile Fan converge southward with the older late Pleistocene alluvium which forms most of the upper fan surface. Bouldery Holocene alluvium, which spread across the lower central part of the Fortymile Fan in the vicinity of U.S. Highway 95 to a width of about 3 km, is characterized by a recognizable depositional morphology and weakly developed soils. The thickness of this recent alluvium generally is not exposed. However, in one borrow pit near U.S. Highway 95, the alluvium is about 3 to 4-m thick and lies above a buried soil. The latter may mark the top of a late Pleistocene alluvial unit associated with fanhead incision in yet older, unexposed alluvium occurring from about 40 to 25 ka.

During the Holocene and especially during the transition to the Holocene (about 15 to 8 ka), hillslope erosion supplied sediment to Fortymile Wash, which aggraded over its lower reach. Analysis of Holocene alluvium indicates erosion of an average of at least 60 cm of colluvium on Yucca Mountain (or about 18 cm of bedrock equivalent) eroded over the past 15 ky, but it is not known what quantity was transported into Fortymile Wash. Local hillslope erosion at Jake Ridge by a high-intensity convective storm in July 1984 supplied sediment to Fortymile Wash (Coe and others, 1995).

Most major tributaries to Fortymile Wash have supplied young sediment to Fortymile Wash as seen, for example, by young tributary fans built into and truncated by Fortymile Wash. Further, the downwash decrease in the portion of basaltic clasts in young Fortymile gravel is due to dilution by non-basaltic alluvium from tributary drainages below upper Fortymile Canyon (Lundstrom and Warren, 1994).

Aggradation during sediment transport events along Fortymile Wash is an expected consequence of streamflow infiltration along the channel. The downwash decrease of peak flows due to infiltration was documented for events in 1984 (Savard and Beck, 1994). Infiltration along Fortymile Wash is a major component of a regional infiltration model based, in part, on channel morphology. The geochemistry and distribution of apparent age of ground water beneath the fan of lower Fortymile Wash indicates that this process also was important during transition to the Holocene (Claassen, 1985).

Channel infiltration and sediment deposition is magnified where the young Fortymile Wash alluvium spreads out as a fan over the older surface (the intersection point). The intersection point reflects a erosion of hillslopes in the lower Fortymile Basin.

Hydroclimatic Implications of Fortymile Wash History

Fortymile Wash in today's climate is extremely ephemeral. Flow in the wash has been observed during parts of less than 30 days over the past 27 years anywhere along its main channel from Buckboard Mesa southward to its confluence with the Amargosa River channel. However, Fortymile Wash probably had perennial or sustained seasonal flow along at least portions of its length during wetter climates over the past 100 ky. In particular, perennial or at least seasonally sustained flow through Fortymile Canyon seems likely to have occurred from about 50 to 25 ka when the fanhead was being incised. In central Fortymile

moisture. However, the modern water table nears the fan surface southward and near the Stateline area. Samples from the spring discharge areas at the toe of the Fortymile Wash alluvial fan yield dates indicating the water table intersected the surface during the last two glacial periods.

Aggradation in Fortymile Wash resumed around 15 ka when climate was in transition towards the interglacial (Holocene) period. That episode of aggradation continued until about 8 ka and then largely ceased in a modern-like, very dry climate. Paradoxically, human artifacts occur along stretches of Fortymile Wash, and they seem to indicate a human presence that may indicate at least some episodes of seasonal flow. However, no aggradation associated with that potential flow has been identified.

[redacted]

and/or waters permit estimation of temperature of mineral formation or isotopic ratio of the mineral's source water. In the case of the secondary minerals found in open spaces and on fractures within the UZ, the $\delta^{18}O$ values of infiltrating waters were estimated from the $\delta^{18}O$ values of calcite ($CaCO_3$) and/or opal ($SiO_2 \cdot nH_2O$). Inasmuch as the $\delta^{18}O$ of the infiltration directly reflects meteoric waters, these studies provide the only linkage between past precipitation (air-mass source) and UZ hydrology.

Secondary calcite carbon ($\delta^{13}C$) values in the UZ reflect the isotopic values of dissolved carbon species in the percolating waters and acquired within the soils during infiltration. Soil carbon dioxide generally arises from the oxidation of organic soil matter derived from the resident plant community. That CO_2 has a $\delta^{13}C$ value directly related to the ratio of plants using the C3 photosynthetic pathway to these using the C4 pathway. The C3 plants dominate under cooler and wetter climates (such as those of Pahute and Rainier Mesas near Yucca Mountain) and have $\delta^{13}C$ values near –25 per mil. The C4 plants are better suited to hotter and drier climates such as that of Crater Flat and have $\delta^{13}C$ values near –13 per mil (Quade and others, 1989). Calcite $\delta^{13}C$ values, therefore, reflect the overlying plant community and provide information about the climate supporting these plants.

Isotopic studies of SZ calcite indicate it formed largely as an alteration phase during moderate temperature hydrothermal alteration roughly 10.5 Ma (Broxton and others, 1987; Bish and Aronson, 1993). Therefore, they provide little, if any, information pertinent to reconstruction of past climates and are not discussed further.

Initial studies of UZ secondary minerals, however, concluded much of this record was deposited within the past 350 ky, some as recently as 26 ka (Szabo and Kyser, 1990). Szabo and Kyser (1990)

[redacted] the recent hydrologic response of the UZ to climate variability.

Secondary Mineral Parageneses

Study of mineral assemblage textures (macro- and microscopic) establish the physical and temporal (paragenetic) relation between different mineral phases or successive mineral assemblages, thus providing hydrological evidence of their origins. Secondary mineral textures from UZ occurrences indicate that at least two major periods of mineral precipitation are common: an early period, predominantly composed of the silica phases quartz, chalcedony, and possibly opal with minor calcite and sparse, local fluorite, and a second period involving mostly calcite and opal. This early stage may include mineralization formed during tuff cooling or under a higher geothermal gradient. The later stages of mineralization largely produced calcite but also produced spatially and temporally common occurrences of opal. Fluid inclusion (Roedder and others, 1994) and stable carbon and oxygen (Whelan and others, 1994) data are completely consistent with formation of this later calcite from dilute, low-temperature meteoric waters percolating through the UZ during the Quaternary.

Scanning-electron and plane-light microscopic observations indicate the UZ calcite and opal probably did not co-precipitate. Several occurrences, however, indicate multiple, cyclic, fine-scale depositional couplets of late calcite and opal that likely reflect short-term control by climate and/or UZ hydrochemistry (J.F. Whelan, R.J. Moscati, S.B.M. Allerton, and B.D. Marshall, U.S. Geological Survey, written commun., 1996).

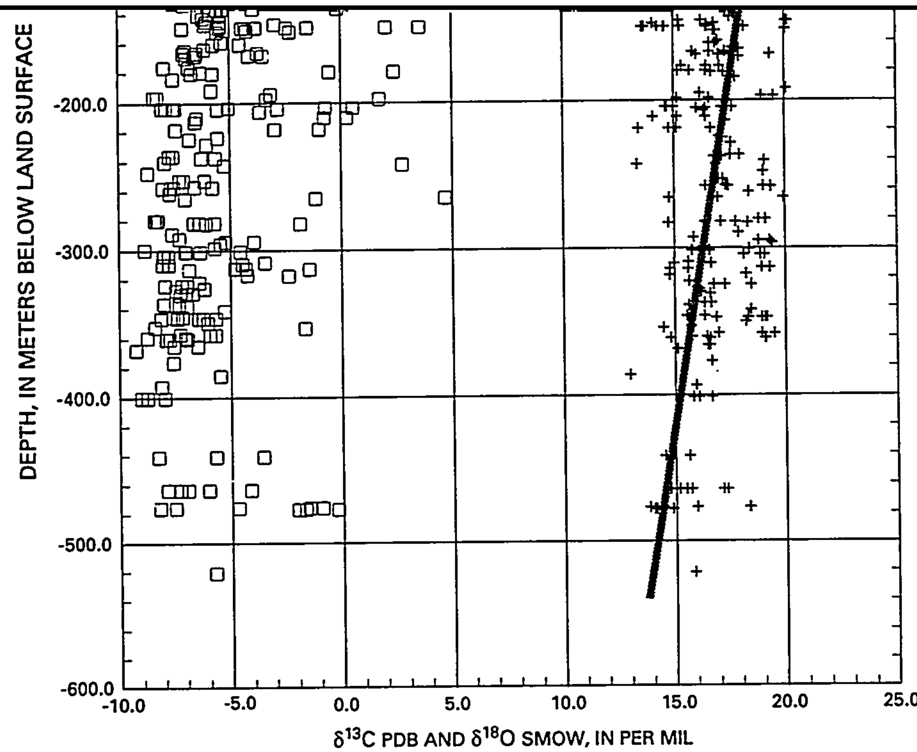

Figure 15. Plot of $\delta^{13}C$ (squares) and $\delta^{18}O$ (crosses) values of calcite versus depth (m) within the unsaturated zone. The line is the predicted $\delta^{18}O$ of calcite precipitated along a hypothetical geothermal gradient of approximately 34°C/km from a fluid with a $\delta^{18}O$ of about −12.5 per mil.

Isotopic Geochemistry of Unsaturated-Zone Secondary Calcite

Within the UZ, later stage calcite $\delta^{13}C$ values generally are between −9 and −3 per mil (fig. 15) but range up to +8 per mil; $\delta^{18}O$ values range from 12 to 21.5 per mil and display a regular decrease with depth. The $\delta^{13}C$ range indicates large variations in the past carbon isotopic composition of CO_2 in the soil zone. Figure 16 shows that approximately 60 percent of the $\delta^{13}C$ values fall between −8 and −4 per mil, with a pronounced mode around −6 ± 2[2]. This range is essentially identical to that of calcretes on and around Yucca Mountain (J.F. Whelan, U.S. Geological Survey, written commun., 1997). Quade and Cerling (1990) concluded these calcretes formed during colder and wetter climates than today and probably are comparable to the flanks of the modern Rainier Mesa. Such values, therefore, imply calcite deposition within Yucca Mountain occurred during colder and wetter climate periods that supported increased levels of infiltration and fracture flow relative to today. Detailed microsampling of the fine laminae within Yucca Mountain may provide a $\delta^{13}C$ stratigraphy linking the long-term history of plant communities to percolation and calcite deposition and, hence, insight to the history of water flux in the UZ.

---

[2] Most of the higher $\delta^{13}C$ values in figure 16 probably represent mechanical mixtures of early-stage calcite, with values as high as +8 to +9 per mil, and the later stage calcite, with values near −6 per mil.

[redacted]

(fig. 15). Meteoric water $\delta^{18}O$ values are a function of air-mass trajectory and moisture source. Modern extremes of precipitation $\delta^{18}O$ values in the Yucca Mountain region, for instance, range between arctic

[3]Fairly good agreement between the total ranges predicted for 100 m (–15.7 to –8.5 per mil) and 500 m (–14.5 to –8.5 per mil) supports use of the measured geothermal gradient (Sass and others, 1980) for past reconstructions.

Comparison between the calculated $\delta^{18}O$ ranges of past infiltration water and the typical $\delta^{18}O$ values of modern air masses determined by Benson and Klieforth (1989) indicates that most UZ calcite has precipitated from waters derived from rain or snow produced from some mix of maritime and continental polar and arctic sources. The highest water $\delta^{18}O$ values of about −8 per mil may reflect evaporation of infiltrating waters or record infiltration during a past climate with a subtropical source water, as would occur if the present summer circulation were intensified.

Climate states producing the most calcite, however, are not necessarily those producing the greatest UZ flux. Wetter climates that produced greater fluxes, but which were calcite-undersaturated and left no mineral record, are certainly possible. Additional geochronologic studies are needed to delimit those climate states conducive to calcite-depositing percolation.

Conclusions

1. Later-stage secondary calcite and opal formed from percolation of meteoric waters through the UZ and display oxygen and carbon isotopic signatures from those waters and soils. Early-stage calcites do not appear to be related to climate processes.
2. Both carbon and oxygen isotopic signatures indicate that calcite-depositing percolation occurred during climates colder and/or wetter than today—calcite-depositing climates, however, are not necessarily the wettest climate states of the past 400 ky.
3. Understanding the relation between past climates and UZ hydrology will be enhanced with more precise determinations of the timing of episodes of secondary mineral formation.

Linkage Between Paleohydrology and Strontium Isotopes

Strontium isotopic values are ideal solute tracers and, because strontium is chemically similar to calcium, it is a common minor element in calcium-bearing minerals. Calcite ($CaCO_3$) and other carbonate minerals commonly incorporate and fix strontium when they precipitate from waters. Unlike isotopes of lighter elements, strontium isotopes do not fractionate significantly as a result of geochemical or biochemical processes. The pertinent strontium isotopic data will be discussed first in the SZ records and then in the surficial soil environment that influences the infiltration and UZ records.

Calcite mineralization provides one of the key records of paleohydrology. Secondary accumulations of calcite, in the form of spring deposits or as infillings in bedrock, are measured to determine the strontium isotope composition of the water at the time of mineral precipitation to provide information about solute sources. The strontium isotopic compositions of these calcite deposits directly record the isotopic composition of ancient waters. Dating the calcite deposits with uranium-series and radiocarbon methods provides a linkage between paleohydrological records and climate.

The strontium isotopic values in water are determined by the geology of the recharge area and, to a lesser extent, by water-rock interactions along the flow path. Once chemical equilibrium between the rock and water is established, further reactions that could change strontium isotopic values are diminished. In order to assess the variation in $^{87}Sr/^{86}Sr$ in ground water with time, samples of carbonate from Devils Hole spring (Winograd and others, 1992), which have been dated by Ludwig and others (1992), were measured. Six samples of this carbonate deposited at 650 to 180 ka show variation in $^{87}Sr/^{86}Sr$ (fig. 17; Marshall and others, 1990). This variation is most likely due to changes in the relative amounts of recharge through the variable geology at higher elevation. This example shows that strontium isotopes can vary in a flow system due to changes in climate and that the magnitude of this variation is relatively small.

The Saturated Zone at Yucca Mountain and Changes in the Water-Table Position

Fracture- and cavity-filling deposits within the volcanic rock section at Yucca Mountain commonly contain calcite. The strontium isotope compositions of these calcite deposits are plotted in figure 18. In general, the physical, chemical, and isotopic parameters of these calcites correspond to their locations within either the SZ or UZ (Marshall and others, 1992). These parameters all indicate different origins for these two groups of secondary calcite.

Present-day ground water beneath Yucca Mountain, with mean $^{87}Sr/^{86}Sr = 0.7107$ (Marshall and others, 1992), cannot be the source of the strontium in the SZ secondary calcites, which contain strontium

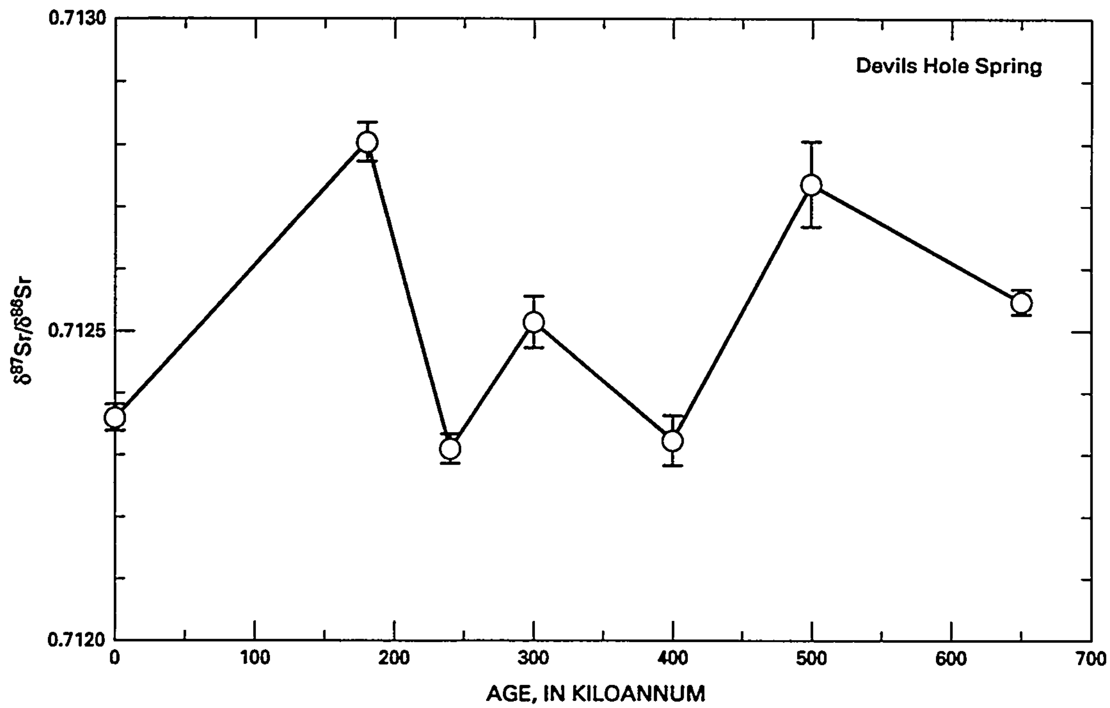

Figure 17. Strontium isotopic composition of calcite deposited at Devils Hole spring, Nevada, plotted as a function of age. The zero age point is the composition of the current discharge. The total range of strontium-87/86 shown here is much smaller than the range of any sample groups.

with an isotopic composition characteristic of Paleozoic carbonate rocks ($^{87}Sr/^{86}Sr$ = 0.708 to 0.709; fig. 18). These values imply water from the deeper regional carbonate aquifer penetrated upward into the volcanic rock section, probably early in the history of the volcanic rocks, and deposited calcite. There are currently no reliable age data to support or refute this hypothesis for the origin of the SZ calcites.

Discharge sites active within the Quaternary are found about 20 km southwest of Yucca Mountain, indicating that the water table (or a perched table) was at the surface in the past (Paces and others, 1993; see also discussion below under Past Ground-Water Discharge). Strontium isotope compositions ($^{87}Sr/^{86}Sr$ = 0.713) of carbonate from these sites are fairly atypical for the Yucca Mountain area (Marshall and others, 1993), but those values are known from one well in Crater Flat.

Today, the water table is about 100 m below ground surface near the past discharge sites. Because the discharge sites are most likely the result of a regional water-table rise, the water table would also have been higher at Yucca Mountain when the discharge sites were active. There are multiple lines of evidence pertaining to a higher water table at Yucca Mountain (Marshall and others, 1993). Eighty-five meters above the water table, the UZ secondary calcite contains strontium with an isotopic composition similar to present-day ground water. Although these calcite samples are not unique in other parameters, their strontium isotope ratio is indicative of an origin unlike that of the bulk of the UZ calcite. The strontium data clearly indicate distinct origins for the UZ and SZ calcites and indicate that the present water-table position may have been approximately 85 m higher in the recent past in order to explain the $^{87}Sr/^{86}Sr$ values of the four G–2 samples from the UZ.

Perched water has been encountered in many boreholes at Yucca Mountain. It contains strontium with an isotopic composition identical to that in the pedogenic calcite discussed below (Marshall and others, 1994). Therefore, the perched water is not a remnant of an ancient higher water table. The perched water is probably locally derived during times of higher infiltration than the present day.

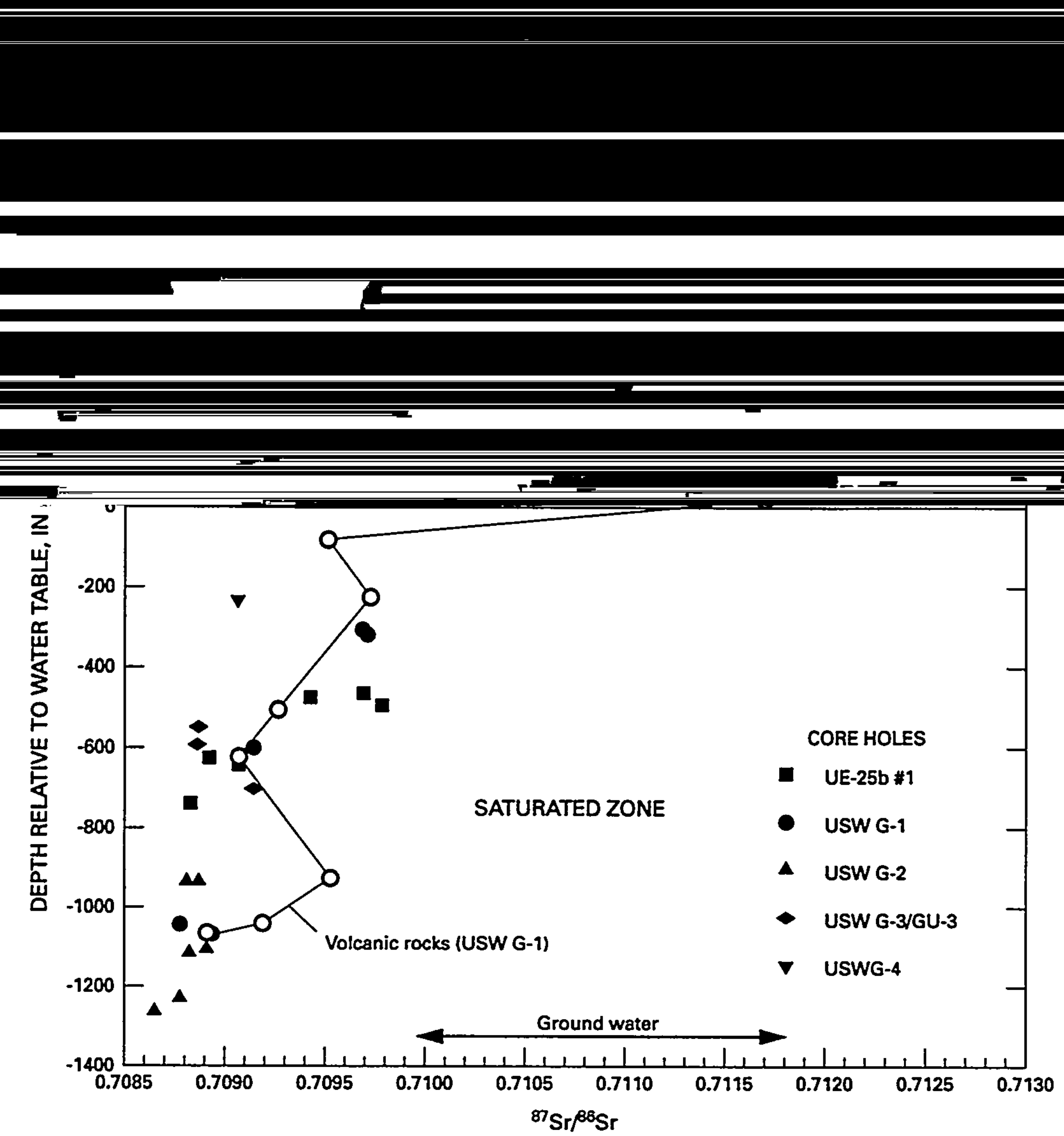

Figure 18. Strontium-87/86 ratios in calcites from various core holes as a function of depth relative to the depth of the water table in the core holes sampled. The histogram at top shows the range of data for pedogenic calcites. Composite samples of the volcanic rocks from borehole USW G–1 are shown for comparison. The range of $^{87}Sr/^{86}Sr$ values in ground water in the vicinity of Yucca Mountain, Nevada, is shown by the double-headed arrow at bottom.

Pedogenic Calcite at Yucca Mountain

Calcite is present in the surficial environment in the form of coatings on bedrock surfaces, calcretes within soil horizons, and vein calcretes within fault zones. Ultimately, all of these occurrences of calcium carbonate derive their calcium primarily from an eolian source (Marshall and Mahan, 1994). Porous sediments in soils of arid and semiarid regions usually require an allogenic component for the source of the large amounts of calcium carbonate (Machette, 1985). Strontium isotopes in calcic soil horizons (K horizons) obtained from calcretes and rhizoliths have values of $^{87}Sr/^{86}Sr$ (0.7117 to 0.7127) that are virtually identical to those of calcite in eolian sediments, surface coatings, and soil A/B horizons. Therefore, the model proposed for the pedogenic carbonate (fig. 19) starts with the eolian component as an end-member composition. However, there are two problems with this hypothesis: (1) The samples taken as typical of eolian materials may be poor proxies for the dust flux today or in the recent past, and (2) only a few materials exist with more radiogenic $^{87}Sr/^{86}Sr$ required to explain the strontium values of the pedogenic calcite. Analysis of pedogenic carbonate silicate residues and comparison with the $^{87}Sr/^{86}Sr$ values of the volcanic rocks in the Yucca Mountain area did not reveal the more radio-

The eolian sediment directly forms surface coatings on   activity that differs from the modern climate.

[redacted]

calcites derive their strontium from pedogenic carbonate exposed at the surface. The decrease in $^{87}Sr/^{86}Sr$ values with depth in the UZ may reflect an increasing input from volcanic feldspar with depth, that is, the lowest $^{87}Sr/^{86}Sr$ UZ ratios derive most of their strontium from pore water in the tuff. The UZ secondary calcite and opal, thus, are directly related to surficial deposits that, similar to the stable isotopes, demonstrate the existence of surface-derived percolation within the UZ, presumably as a function of climate change.

Conclusions

1. Strontium isotopes are an ideal tracer of the solute sources in surface and ground waters and are a common component of calcite.
2. Strontium in ground water can vary in its isotopic ratio over time but within a limited range.
3. Calcite fracture/cavity fillings within the SZ at Yucca Mountain are probably very old and are not in Sr isotopic equilibrium with present-day ground water.
4. Calcite deposited at past discharge sites has a distinct Sr isotopic composition that can be linked to ground water at Crater Flat.
5. There is evidence for an extension to Yucca Mountain of the ancient higher water table that existed at the discharge sites.
6. Perched water has a Sr isotopic composition consistent with derivation from local infiltration rather than an older, higher water-table stand.
7. In general, calcite in soils and within the UZ is consistent with derivation from eolian sources, but evidence shows that these sources may vary in time, possibly reflecting different past climates.
8. Unsaturated-zone fracture fillings record infiltration and percolation of surface water that obtained Sr from soil carbonate. There is little evidence for interaction with the volcanic rocks.

A key remaining issue in determining the suitability of Yucca Mountain for the construction of a potential nuclear-waste repository centers on the past, present, and future water flux through the repository block. Characterization and understanding of the modern UZ hydrologic system is critical to the flux issue, but no matter how complete this understanding, it is but an instantaneous hydrogeologic observation in a temporal continuum of change. Therefore, deciphering the paleohydrology of the UZ is requisite to understanding how water fluxes may vary in the future in response to climate change. Fortunately, mineralogical records of past percolation exist in the rock mass, and these can be used to estimate fluxes by establishing a statistically and spatially valid distribution of ages of these minerals.

Low-temperature secondary minerals, notably calcite ($CaCO_3$) and opal ($SiO_2 \cdot nH_20$), were deposited in open fractures and cavities in the volcanic rocks at Yucca Mountain by water percolating downward through the UZ over long periods of time. Through their contained radioactive clocks ^{14}C and U-series disequilibrium isotopes, the depositional history of these minerals can be established. Calcite also contains isotopic records (O, C, and Sr) that link infiltration and depositional history with climatic variations at the surface; these data are discussed elsewhere in this report. The spatial and temporal distribution of isotopic ages, coupled with estimates of the abundance and spatial variability of calcite and opal in the Exploratory Studies Facility (ESF), will be used to estimate the flux required to produce this physical record of percolation. An understanding of how the flux responds to changing climatic conditions at the surface will be developed from both the resulting temporal framework and from the isotopic records contained within calcite. Lack of correlation between the depositional (or dissolutional) history of the subsurface mineral records and changing climate would testify to the long-term stability of a system that was effectively buffered from external hydrological forcing factors (Chapman and McEwen, 1993).

The incorporation of uranium and the virtual exclusion of thorium from both calcite and opal when

The magnitude of these effects on the determined ^{14}C ages is presently not known. The mere presence of detectable ^{14}C in a sample implies formation of calcite within the last 40 ka, even if exact ages cannot be determined.

A parallel study also aimed at developing a better understanding of past water flux is being conducted by Los Alamos National Laboratory using chlorine-36 ($^{36}Cl/Cl$) measurements (J. Fabryka-Martin, A.V., Wolfsberg, P.R., Dixon, S., Levy, J., Musgrave, and H.J., Turin, Los Alamos National Laboratory, written commun., 1996). Salts, formed by the evaporation of pore water, are extracted by leaching with deionized water, and the $^{36}Cl/Cl$ ratios are measured by accelerator mass spectrometry.

Sampling and Analyses

The ESF provides a unique opportunity to study and sample calcite and opal deposits in the potential repository rock mass. Delicate crystal forms are well preserved in both lithophysal cavities and in open fractures. Such features were not seen in drill core, apparently because they were destroyed during the drilling process.

Because of potentially low depositional rates, microsampling was conducted with dental tools and small grinders under a microscope to acquire a sample representing a minimal stratigraphic thickness. Even with this fine-scale sampling approach, the samples likely do not represent finite growth or depositional intervals (J.B. Paces, U.S. Geological Survey, written commun., 1996). Sampling resolution ultimately is limited by analytical requirements of 10 to 20 mg of calcite for ^{14}C analyses, whereas U-series analysis requires 50 to 100 mg of calcite and 0.1 to 2 mg of opal. The very small sample size required for opal is a result of relatively large U contents (typically 50 to 200 ppm). The net effect of sampling over multiple growth layers is that the determined ages ($^{230}Th/U$ and ^{14}C) will be biased somewhat toward the young side of the true mean age of the material. Where multiple subsamples have been taken from a single sample, the isotopic ages are consistent with relative ages established from mineral relations. The age data also clearly demonstrate that these occurrences formed by very slow depositional rates on the order of micrometers per thousands of years.

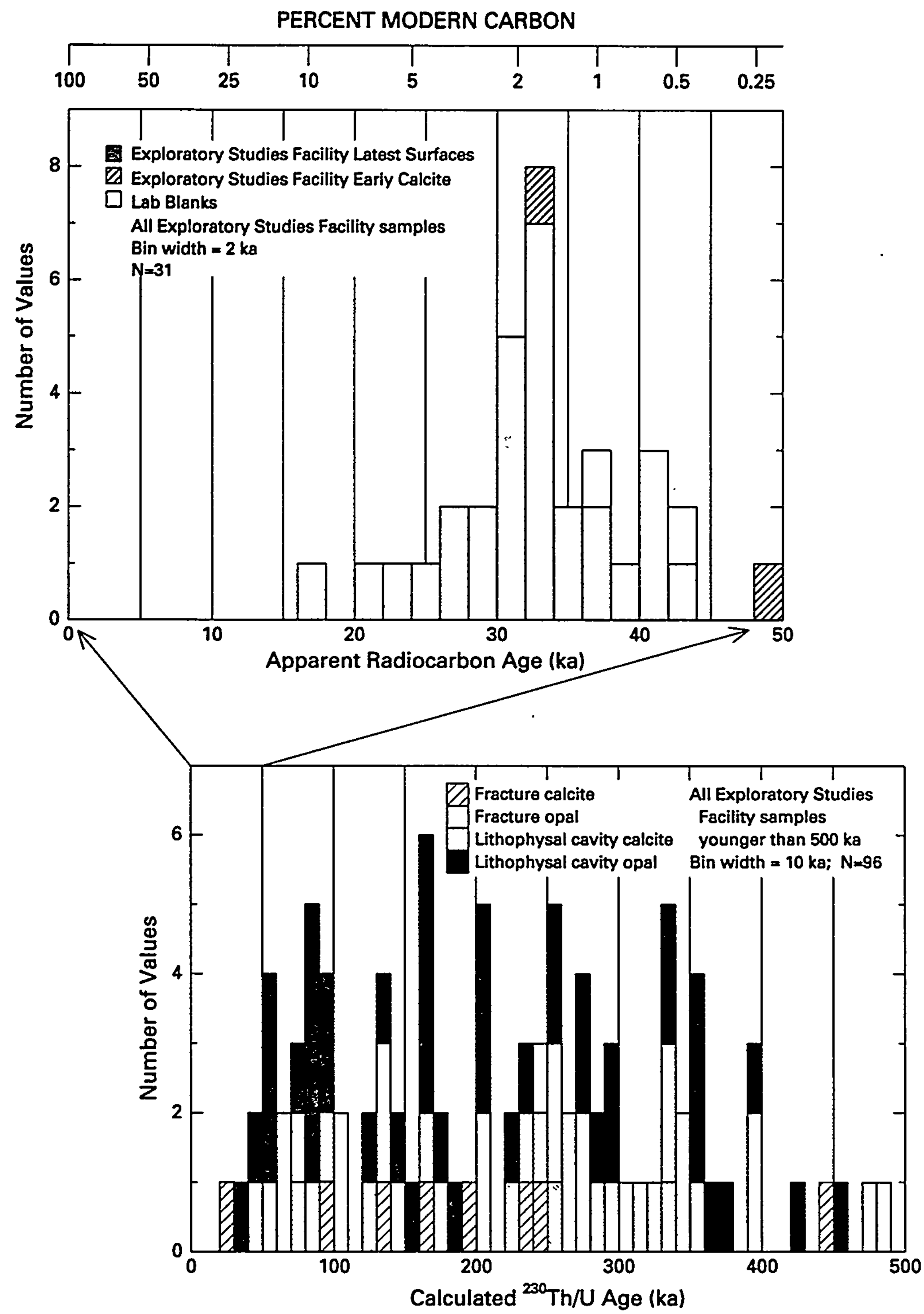

Figure 20. Histograms of apparent radiocarbon and ^{230}Th/U ages determined from calcites and opals from the Exploratory Studies Facility, Yucca Mountain, Nevada. Note tenfold difference in age scale between upper and lower histograms. Most age determinations are from materials representing outermost growth surfaces. Data have been interpreted to represent very slow rates of mineral deposition (J.B. Paces, written commun., 1996), with the possibility of mechanical mixing between younger and older components within a single analysis.

from a fracture, and the oldest ages within the 500 ka range (which is the approximate limit of the technique) are on opal at 470 and 480 ka. On the assumption that any age bias resulting from sampling material deposited over finite time intervals is minimal, a correlation between age distribution (time of mineral deposition) and climatic cycles might be expected. Proof of such a correlation will require a statistically valid number of age determinations in order to delineate clearly depositional and nondepositional episodes should they exist.

When the ESF dating study has been completed through the southern part of the main drift and through the south ramp, the geochronologic data base should be sufficiently large for a reliable assessment of

great importance to the issue of radioactive waste isolation in the potential geological repository at Yucca Mountain.

The potential repository horizon is located approximately 200 to 400 m above the present-day water table. However, evidence for higher SZ water levels at some time in the past has been derived from secondary mineral occurrences (Levy, 1991) and Sr isotopic variations (Marshall and others, 1993) from borehole data, and from hydrologic models involving increased recharge (Czarnecki, 1985) in the Yucca Mountain regional flow system. Although evidence from these studies indicates a maximum increase in water-table elevation of 100 to 150 m, the age of these fluctuations remains unconstrained.

more spatially restricted but include the high-volume springs at Ash Meadows and in Death Valley, as well as wide-spread seepage discharge at Franklin Lake Playa. All of these paleodischarge deposits have low-lying, badland-type morphologies with lithologies dominated by whitish-gray to pale-green, sand- and silt-rich detritus. Coarse clastic material is conspicuously absent, a feature that readily distinguishes them from alluvial and colluvial deposits associated with surface-water transport (Quade and others, 1995). Bedding is typically massive, punctuated by laterally discontinuous layers of authigenic materials such as carbonate-rich nodules or mat-like layers containing casts of insect burrows or plant petrifactions. Authigenic calcite and lesser silica produce a wide range of cementation from soft, barely calcareous silt to contorted hard nodules to dense limestone containing regularly spaced, subvertical tube-like voids (probably plant-stem molds). Much of the layered or nodular limestone typically contains fine-grained siliciclastic material (clays), which complicates ^{230}Th/U geochro-

able upper age limit is determined, in part, by the initial $^{234}U/^{238}U$ ratio, where the higher the initial ratio, the older the detectable age. The detectable upper age limit also is a function of the analytical precision, where the better the precision, the smaller the error range and the greater the ability to resolve older ages. Young ages are more common due to those materials being readily accessible at the surface. Ages, shown in figure 22, are plotted against the calculated initial $^{234}U/^{238}U$ (value of $^{234}U/^{238}U$ in the discharge water at the time of mineral formation). No systematic trend of initial $^{234}U/^{238}U$ versus age is apparent in these data. Indeed, nearly the entire range of initial $^{234}U/^{238}U$ variation, from approximately 3 to 4.5, is observed in the youngest materials (20 to 10 ka). The wide range of calculated initial $^{234}U/^{238}U$ is interpreted to reflect real variations in water compositions during the latest episodes of discharge. Uniform calculated initial $^{234}U/^{238}U$ for samples with older ages provides an internal check of the accuracy of the ^{230}Th/U ages.

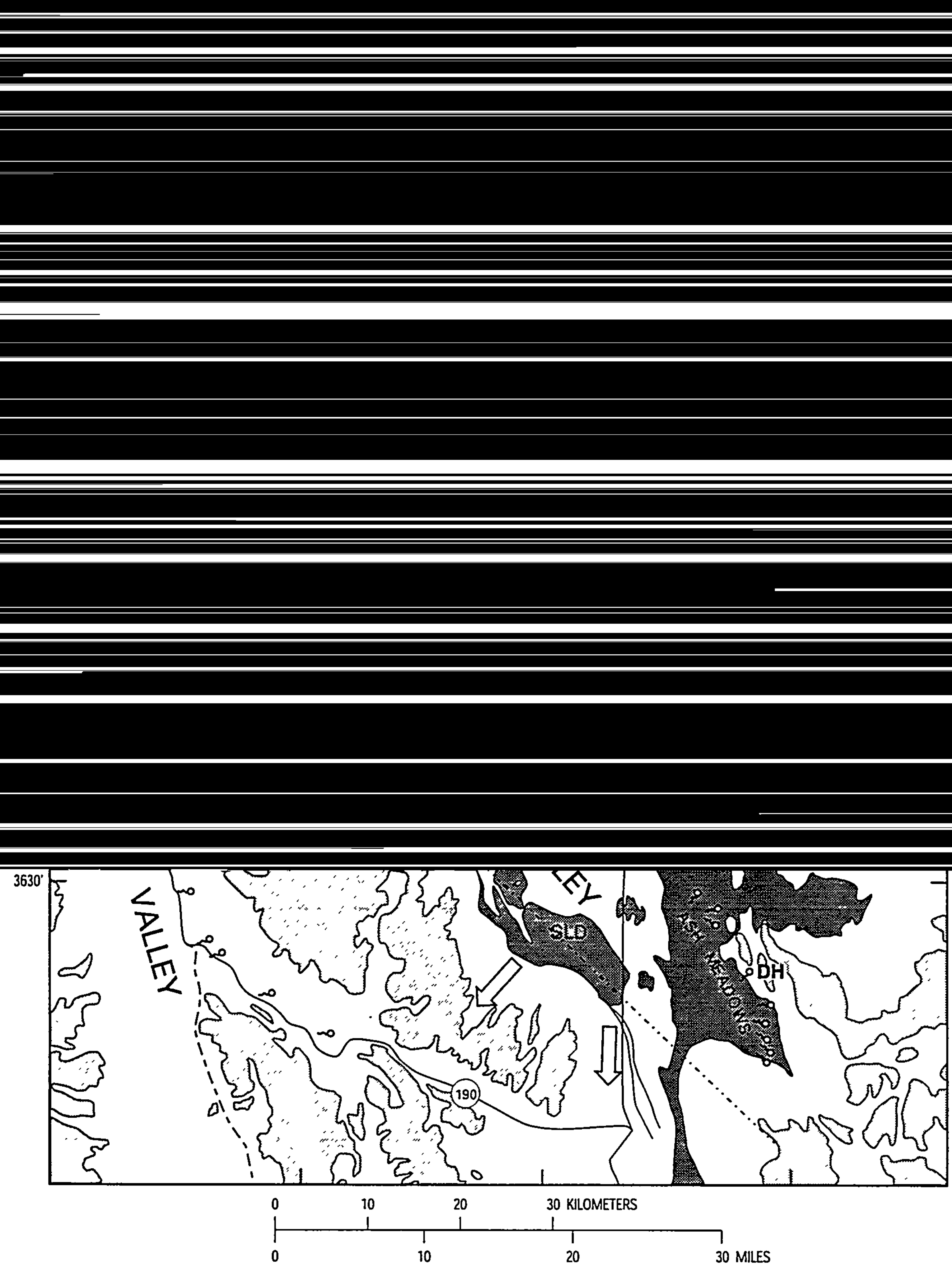

Figure 21. Paleodischarge deposits [dark-shaded patches with CFD = Crater Flat Deposits, CFW = Crater Flat Wash, DH = Devils Hole, LWD = Lathrop Wells Diatomite, IPD = Indian Pass Deposits, SLD = State Line Deposits in the Yucca Mountain region, Nevada. Active springs at Ash Meadows and Death Valley are shown with spring symbols. Outlined arrows show generalized ground-water flow paths. Light-shaded polygons represent bedrock highs; intervening unpatterned areas represent alluvium-filled basins. Solid and dashed lines in basins represent fluvial channels and fan boundaries, respectively.

near the base of the exposed Lathrop Wells Diatomite

determined from the silt fraction in the same sediment.

[redacted]

major lithologic break yielding ^{230}Th/U ages from the last and penultimate glacial cycles. The reason for this age discrepancy is unclear. In contrast, the lowermost fine-sand unit dated by TL at the State Line high-terrace deposits yields a TL age of about 120 ka,

young ages obtained using the three independent methods strongly indicates a primary age signature rather than partial resetting of older deposits by younger processes (that is, climate-induced pedogenic overprinting).

hydrologic condition (see discussions under the Owens Lake, Lakes, Playas, and Marshes, and Terrestrial Records sections of this report).

- The ^{230}Th/U data show discharge activity was cyclic and associated with the last and penultimate glacial cycles. Deposits from the penultimate glacial cycle are exposed only in the more deeply dissected sites at the Lathrop Wells Diatomite deposits and State Line deposits, with the possibility of older materials at the base of a shallow (1.5 m) pit at the Crater Flat deposits. Elsewhere, the older deposits are not exposed, have been removed by erosion, or have not yet been identified.

- Materials younger than about 16 to 10 ky old have not been identified from any of the sites, including surface-lag deposits that form as these badland-type deposits are deflated. The absence of Holocene material indicates that the last discharge activity ceased around 15 to 12 ka at upgradient sites and slightly later (about 9 ka) downgradient at lower elevations (as at the State Line deposits). This time corresponds to the cessation of the last cycle of spring activity in the Las Vegas and Pahrump Valleys (Quade and others, 1995) and reflects initiation of the hotter and dryer conditions typical of much of the Holocene interglacial interval.

Paleontological Data and Paleoenvironmental Conditions

Paleontological analyses of ostracodes, molluscs, and diatoms from samples collected from the Lathrop Wells Diatomite deposits, the Crater Flat deposits, and the Amargosa River site at the State Line deposits show that discharge was common in the past and supported a variety of discharge-related paleoenvironments. These paleoenvironments may be generally classified as seeps, flowing springs, and spring-supported standing water (shallow pools and wetlands).

Paleoecological evidence indicates that seeps were common. These environments are characterized by low levels of ground-water discharge, minor surface-water flow, high seasonal variability of water temperature, and probable variation in water chem-

istries had low to moderate seasonal variability that likely was inversely proportional to discharge flux. Spring-supported pools and wetlands also were common in the region, particularly near the modern-day Amargosa River. These open-water environments must have varied from a few meters in diameter to shallow ponds or lakes hundreds of meters in diameter. These environments were variously permanent or ephemeral. Dense stands of emergent aquatic vegetation (cattails, bulrush), grasses, or other vegetation occurred at these sites.

Paleoenvironmental reconstruction at the Lathrop Wells Diatomite paleodischarge site based on analyses of diatoms indicates the presence of a freely flowing alkaline spring system, probably with multiple spring orifices discharging throughout the history of activity. The spring water was silica-rich, only slightly saline, and possibly warm. Its chemistry probably resembled water from the volcanic aquifer. Spring flow was typically moderate to strong and probably passed through a mass of rush-like vegetation that grew at the site.

Stable Isotope Data

Stable carbon and oxygen isotopes in carbonates from paleodischarge sites provide information on the source of the discharging water ($\delta^{13}C$) and the temperatures at which recharge and discharge took place ($\delta^{18}O$). Paleodischarge deposits near Yucca Mountain are often carbonate-poor, unlike other springs in southern Nevada where discharge comes from deep, carbonate-hosted aquifers. Carbonate-poor deposits could be due to discharge waters with little capacity to precipitate calcite. This could be due to (1) dilute, calcite-undersaturated discharge waters; or (2) calcite-saturated, but calcium- or carbonate-poor waters.

Stable isotope data from the five paleodischarge sites show a large range in both $\delta^{18}O$ values (18 to 27 per mil) and $\delta^{13}C$ values (–10 to +1 per mil) (fig. 23). These $\delta^{13}C$ and $\delta^{18}O$ values also show positive covariance, indicating evaporation and CO_2 escape from discharge waters at the surface. The smallest inorganic carbonate $\delta^{18}O$ values, representing materials least affected by surface processes, cluster around 19 ± 1 per mil. The range of $\delta^{13}C$ remains large even for carbonates with minimum $\delta^{18}O$ values, a feature that reflects mixing between the primary either evaporated and/or lower-temperature waters.

Minimum $\delta^{18}O$ values of carbonate from each deposit most closely reflect the temperature and isotopic ratios of the discharging waters. At the carbonate-poor, fine-grained marsh and wetland paleodischarge deposits, these minimum $\delta^{18}O$ values are roughly 3 per mil higher than those from the carbonate mounds at active sites such as Ash Meadows and Devils Hole. This difference reflects either cooler discharge temperatures or greater discharge $\delta^{18}O$ values, or both, at the carbonate-poor sites. If near-equal discharge $\delta^{18}O$ values are assumed for water for the two types of deposits, then discharge temperatures at the carbonate-poor sites were 0 to 16°C, significantly cooler than the 25 to 35°C modern sites. If near-equal discharge temperatures are assumed, the 3 per mil lower discharge at the carbonate-poor sites probably reflects recharge at lower elevations than the carbonate-depositing sites. Although unlikely, if the carbonate-poor discharge deposits are associated with warm water discharge, the highest $\delta^{18}O$ values also could result from those warm discharge waters cooling as they flowed away from the orifices. Regardless, either cooler temperatures or lower elevation recharge are more compatible with shallower and shorter ground-water flow paths for the carbonate-poor deposits, and this is likely the key difference between them and the carbonate mound deposits.

K.R. Ludwig, L.K. Kwak, L.A. Neymark, K.R. Simmons, L.D. Nealey, B.D. Marshall, and A.W. Walker, U.S. Geological Survey, written commun., 1995). Similarly low values of $^{234}U/^{238}U$ are observed for surface-runoff waters collected during precipitation events at Yucca Mountain. Therefore, data from paleodischarge deposits clearly require a hydrologic source not dominated by surface waters or pedogenic processes

Like U data, Sr isotopes provide additional evidence that a surface-water origin is not feasible. Strontium isotopic compositions of weak-acid leaches largely from the vicinity of the southern Crater Flat and State Line deposits (J.B. Paces, written commun., 1995) yield a bimodal distribution of values based on location. Carbonates from the Lathrop Wells Diatomite deposits and Crater Flat deposits have $\delta^{87}Sr$ values of 5.03 to 5.20, whereas samples from the State Line deposits contain $\delta^{87}Sr$ values between 10.5 and 13.1. Both groups are distinct from local calcretes that have a range of $\delta^{87}Sr$ from 3.3 to 5.0 (Marshall and others, 1993; Marshall and Mahan, 1994).

Carbon from the inorganically precipitated carbonate at all sites contains a substantial component of heavy carbon (–4 and +2 per mil) that is not observed in surface environments where plants control most of the carbon budget. Calcrete throughout the region has $\delta^{13}C$ values of –10 to –5 per mil. Waters

Table 3. Characteristic isotopic compositions of paleodischarge deposits, waters, and rocks representing possible source materials in the Yucca Mountain, Nevada, region.

Material	Initial $^{234}U/^{238}U$ Activity	$\delta^{87}Sr$ per mil	$\delta^{13}C$ per mil
		Paleodischarge deposits	
Inorganic carbonate	2.9 to 4.5	5.0 to 13	−4 to +1
Plant/mollusc	2.9 to 4.5	5.0 to 13	−10 to −5
		Aquifers	
Paleozoic	2.5 to 4	3 to >10	−4 to −2 (HCO_3^-)*
Volcanic/alluvium	3 to 8	-0.7 to 4 (no Precambrian) 7 to >15 (w/Precambrian)	−13 to −7 (HCO_3^-)*
Perched waters at Yucca Mountain	3 to 7	3.5 to 4.5	−11 to −9 (HCO_3^-)*
Surface waters at Yucca Mountain	1.4 to 1.8	1.8 to 3.8	
		Rocks	
Marine carbonate	~1.0	−2 to +3**	−2 to +2
Calcrete	1.3 to 1.8	3.3 to 5.0	−10 to −5
Volcanics	~1.0	−1.3 to 15	Negligible contribution
Precambrian siliciclastics	~1.0	10 to >30	Negligible contribution

*At near-surface temperatures, the equilibrium $\delta^{13}C$ difference between dissolved HCO_3^- and calcite is ~2 per mil.

**In areas of Paleozoic limestone that have been hydrothermally altered, such as Bare Mountain, $\delta^{87}Sr$ values have been elevated from +23 to +30 through addition of radiogenic Sr derived from the Precambrian basement (Peterman and others, 1994).

that obtain their carbon during infiltration through the soil zone will acquire relatively low $\delta^{13}C$ values (−12 to −7 per mil). These $\delta^{13}C$ compositions are widely observed in surface and shallow volcanic aquifer waters beneath Yucca Mountain (Benson and McKinley, 1985) and in UZ carbonates (Whelan and others, 1994, 1996). In contrast, calcite associated with Paleozoic aquifers has $\delta^{13}C$ that reflects marine carbon sources (Coplen and others, 1994; Whelan and others, 1994).

Isotopic attributes of possible source waters as deduced from those of the carbonate spring deposits are permissible with deposition from SZ ground water. Data for ground water sampled from springs and wells throughout the Yucca Mountain region have a wide range of isotopic compositions (table 3), reflecting the isotope geochemistry of the recharge areas and of the aquifers along the flow paths. Uranium isotopic compositions ($^{234}U/^{238}U$) are highly variable in SZ and perched ground-water systems at Yucca Mountain. Published $^{234}U/^{238}U$ activity ratios range from 1.7 to 7.0 (Ludwig and others, 1993) and even larger values have been found in more recent studies. Generally, water samples from the regional carbonate aquifer have $^{234}U/^{238}U$ activity ratios between 1.7 and 3.5 with some exceptions. Ground water in the volcanic aquifer has $^{234}U/^{238}U$ ratios that overlap with those of the carbonate aquifer, but typically extend to values as large as 8.0. Perched ground water at Yucca Mountain has $^{234}U/^{238}U$ activity ratios similar to ground water from the volcanic aquifer. Thus, the $^{234}U/^{238}U$ ratios of 2.9 to 4.5 for calcite spring deposits are mostly in the area of overlapping values for the regional carbonate aquifer and the volcanic aquifer.

Strontium isotopic compositions of ground water from springs and wells in the Yucca Mountain region have $\delta^{87}Sr$ values that range from −0.7 to extremely large values as great as +39.0 (fig. 24, table 3). However, the majority of $\delta^{87}Sr$ values are in the range of 0 to +14, and values for ground water in the volcanic aquifer at Yucca Mountain proper are even more restricted between +1 and +4. Northward from Yucca Mountain, ground-water $\delta^{87}Sr$ values decrease to 0 into the recharge areas and increase southward into the Amargosa Desert to values as large as +11 (Peterman and Stuckless, 1993a). Ground water contacting only Paleozoic carbonate rocks in the regional carbonate aquifer would be expected to have $\delta^{87}Sr$ values in the range of −2 to +3 (table 3) except where the carbonates have been mineralized by

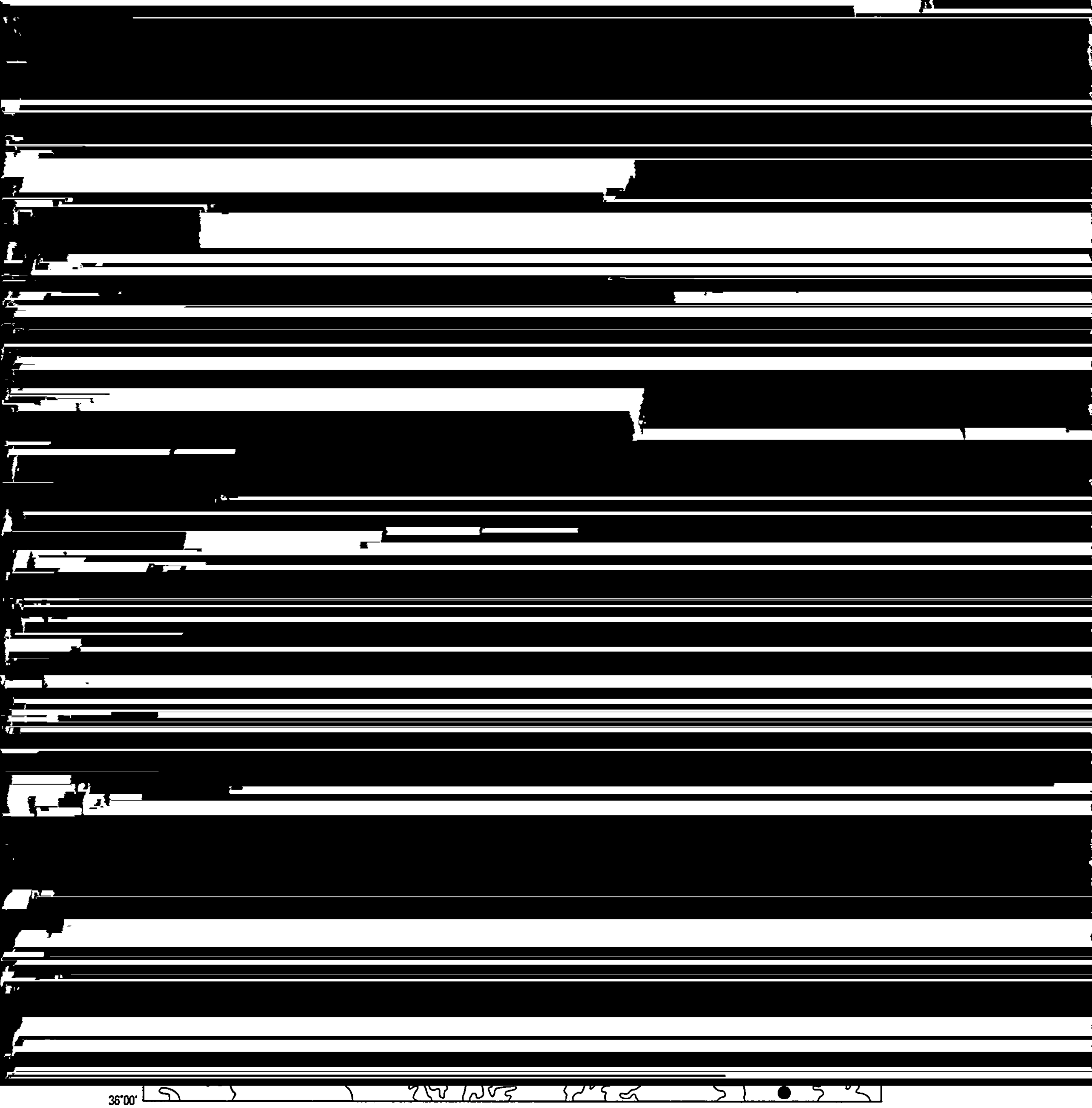

Figure 24. Location of wells and springs analyzed for delta strontium-87 (values in per mil relative to seawater with $^{87}Sr/^{86}Sr$ value of 0.70920) from waters. Bedrock ranges are shown in shaded patterns, and alluvium-filled valleys are shown unpatterned. Solid and dashed lines within alluvial valleys represent active channels and alluvial fan boundaries, respectively. Dark circles represent sample sites classified as Paleozoic aquifer; open circles represent sample sites from volcanic or alluvial aquifers.

siliciclastic units which are the source of the radiogenic Sr. Three springs at the southern end of the spring line have larger δ^{87}Sr values between +11 to +14 (fig. 24), reflecting even greater interaction with Precambrian rocks in the northwestern Spring Mountains.

Possible water sources for the paleodischarge deposits based on isotopic and fossil data are summarized in table 4. Neither perched nor surface-runoff waters will satisfy the isotopic attributes of the spring carbonate deposits. Calcite samples from the Lathrop Well diatomite and Crater Flat deposits have δ^{87}Sr values between +5 and +6 (fig. 24). Ground-water

aquifer. The correspondence between δ^{87}Sr values of the spring deposits and the upgradient ground waters strongly indicates that ground-water discharge occurred at this site and the sites near the southern end of Crater Flat.

Water-Table Fluctuations Under Yucca Mountain

Combined isotopic evidence, including $^{234}U/^{238}U$, $^{87}Sr/^{86}Sr$, and $^{13}C/^{12}C$ as well as spatial and temporal data, indicates that discharging water at paleospring sites represents regional ground waters rather than local perched systems. This conclusion

Table 4. Matrix of possible hydrogenic sources and their compatibility with observed data from paleodischarge sites near Yucca Mountain, Nevada

Hydrogenic source	Initial $^{234}U/^{238}U$ activity	δ^{87}Sr (per mil)	δ^{13}C (per mil)	Diatoms
Paleozoic aquifer	Possible	Possible	Possible	Unlikely
Volcanic/alluvial aquifer	Possible	Possible	Possible	Probable
Perched aquifer	Possible	No	No	No
Surface runoff	No	No	No	No

ated in the past as a response to the higher effective moisture available during wetter climates.

Currently, the water-table elevations beneath the sites closest to Yucca Mountain (Lathrop Wells Diatomite deposits, Crater Flat Wash deposits, and Crater Flat deposits) are extrapolated from potentiometric-surface maps (Waddell and others, 1984; Robison, 1984; Claassen, 1985) because no direct measurements are available. These estimates provide a current depth to water of between 80 and 120 m (Paces and others, 1993). Similar deposits are not found at higher elevation in this area, indicating that these deposits represent a maximum water-table rise over the last 250 ka.

The fluctuations in water-table elevation as recorded at paleodischarge sites may be localized by unidentified hydrogeologic features inasmuch as these deposits are not widespread nor uniformly distributed along areas of equal topographic elevation. However, they probably do not represent the result of an overpressured discharge of a confined aquifer because similar estimates of maximum water-table elevations under Yucca Mountain have been made on the basis of fracture-filling secondary minerals (Marshall and others, 1993) and distribution of zeolitization in tuffs (Levy, 1991). An overpressured system would not produce uniform water-table elevation changes over broad areas. A similar rise in the water-table elevation in the vicinity of the potential repository block at Yucca Mountain (maximum increase of 130 m) also has been modeled using a 15-times increase in recharge responding to doubling MAP relative to modern day (Czarnecki, 1985).

Response of the Water Table to Climatic Variation

One of the main consequences of this work is recognition that higher regional water-table elevations up to 120 m above present-day levels were common during the last two glacial cycles (60 to 10 ka and 170 to 100 ka). The paleodischarge deposits do not contain a continuous sedimentary record like those from lakes. However, the ages obtained thus far do agree with regional climate records (fig. 6); see also discussion above related to Owens Lake. Several important conclusions are apparent from these studies.

records and discharge records implies a direct response of the water table to climate change. There is no apparent lag between the time when climate records identify the availability of surface water to the time when it is observable at discharge sites. This indicates rapid readjustment to increased levels of recharge and translation of the increased recharge downgradient to points of discharge.

Second, much of the late Pleistocene was characterized by higher water-table elevations. Higher water-table elevations may be a normal consequence of Pleistocene climate conditions, and the lower water-table elevations observed today may be typical only of the relatively short, anomalously dry interglacial periods.

Third, multiple climate-cycle histories are recorded at paleodischarge sites, as well as at Devils Hole and Owens Lake. Therefore, water-table elevations as well as regional and local hydrological phenomena have responded to climate change in the past and will continue to do so in the future, which is consistent with studies by Winograd and Doty (1980), Winograd and others (1985), and Winograd and Szabo (1988).

CONCLUSIONS

1. The general features of the climate system, at a millenial scale, can be identified from the timing of insolation change, which is calculated for the past and future. Insolation change occurs in a 400-ky cycle subdivided into four subcycles. A glacial and interglacial couplet are embedded within each subcycle. The insolation characteristics for each glacial/interglacial couplet are not identical, and the corresponding climate characteristics also differ rom one cycle to the next. The timing of insolation change indicates the next glacial cycle will begin within the next few centuries to millennia and the insolation characteristics are most similar to those from the period 400 ka to 350 ka during the glacial period called OIS-10.

2. The well-dated isotopic record of climate change from Devils Hole provides a complete record of the timing of all the glacial/interglacial couplets that have occurred during the past 500 ky. The appearance of glacial periods is essentially the same in both records, but some glacial termination evens occur earlier in the Devils Hole record. The discrepancy in timing between some termination events on the Devils Hole record and in SPECMAP (an integrated marine record of global climate change) may reflect the importance of numerous short-term, earth-based forcing functions on the climate system. Whatever the cause of termination events, the Devils Hole record shows insolation change is not the lone driver or perhaps a driver of those phenomena.
3. The Owens Lake climate record, interpreted from two climate proxy data sets (diatoms and ostracodes), shows a regional expression of all glacial/interglacial couplets from the past 500 ky and indicates the wetter and cooler glacial modes are resident about 80 percent of the time. Further, the characteristics of each glacial/interglacial cycle differ from each other, as does the insolation characteristics of each cycle. The past glacial/interglacial couplet most similar to the insolation characteristics for the next 100 ky, from preliminary interpretation of the Owens Lake record was not as cold as the last two couplets but may have been as wet or wetter.
4. The local aquatic and terrestrial records of climate change during the last glacial cycle (40 to 10 ka) reveal that glacial cycles are climatically complex periods composed of numerous century- and millennial-scale episodes having different climate characteristics. During the last glacial interval, MAP was on average about twice modern, but episodes when MAP was higher are also believed to have existed. Mean annual temperature was typically quite low, commonly around 4° to 5°C, or colder. Effective moisture was nearly always higher than modern during the glacial period due to past combinations of MAP and MAT.
5. Fortymile Wash responded to climate change by variously aggrading or incising portions of the now largely dry wash. During glacial times, the wash appears to have supported a gaining stream in its upper reaches that incised alluvial material near Yucca Mountain. Incision in part may be related to vegetation-stabilized slopes. Conversely, in transition periods from or into a glacial period, the stream aggraded. During dry interglacial periods, the stream remained relatively static with little aggradation or incision.
6. Stable and radiogenic isotope data from calcite and opal formed in fractures within the UZ of Yucca Mountain reveal that those minerals were derived from infiltrating waters. Infiltration appears to have occurred during glacial times, when C3 plants lived in the region indicating colder MAT than today. Calcite $\delta^{18}O$ data indicate the infiltration had isotopic characteristics associated with arctic to maritime polar air if MAT values around 5°C are assumed. A warmer MAT would indicate less input from arctic and more from polar/tropical sources. These data identify the climate characteristics of those percolating waters responsible for calcite formation. Strontium isotopes show a consistent pattern of the percolation solute load derived from the surface, where the strontium, in part, was derived from dissolution of calcretes.
7. Ages of secondary minerals derived from uranium-series and radiocarbon analyses indicate formation primarily, but not exclusively, during glacial periods. Mineral formation primarily during the glacial periods may imply the repository block behaves as a relatively open hydrological system that responds rapidly to climate change.
8. Strontium isoptope data from the present UZ within Yucca Mountain reveal that the regional water table may have been about 100 m higher at some unknown time in the past. Isotopic studies and dating of past discharge deposits down-gradient from Yucca Mountain reveal that during the last and penultimate glacial periods the regional water table rose as much as 100 m, creating wetlands, flowing springs, and seeps from Crater Flat to the Amargosa River. Strontium isotope data from well water link modern Crater Flat ground-water and the nearby ground-water discharge deposits.
9. A positive correlation appears to exist between changes in the 400-ky insolation cycle, climate change, and the hydrologic behavior of the UZ and the SZ within Yucca Mountain.

Basin and Range Province, southern California: U.S. Geological Survey Water-Resources Investigations Report 83–4116–A.

Benson, L.V., and McKinley, P.W., 1985, Chemical composition of ground water in the Yucca Mountain area, 1971–84: U.S. Geological Survey Open-File Report 85–484, 10 p.

Benson, L.V., and Kleiforth, H., 1989, Stable isotopes in precipitation and ground water in the Yucca Mountain region, southern Nevada—Paleoclimatic implications, *in* Peterson, D.H., ed., Aspects of climate variability in the Pacific and the western Americas: American Geophysical Union Monograph 55, p. 41–59.

Berger, A., and Loutre, M.F., 1991, Insolation values for the climate of the last 10 million years: Quaternary Sciences Review, v. 10, p. 297–317.

Bischoff, J.L., 1993, Age-depth relations for the sediment column at Owens Lake, California—OL–92 drill hole, *in* Smith, G.I., and Bischoff, J.L., eds., Core OL–92 from Owens Lake, southeast California: U.S. Geological Survey Open-File Report 93–683, p. 251–260.

Bish, D.L., and Aronson, J.L., 1993, Paleogeothermal and paleohydrologic conditions in silicic tuff from Yucca Mountain, Nevada: Clays and Clay Minerals, v. 41, no. 2, p. 148–161.

Bradbury, J.P., 1993, Diatoms in sediments, *in* Smith, G.I., and Bischoff, J.L., eds., Core OL–92 from Owens Lake, southeast California: U.S. Geological Survey Open-File Report 93–683, p. 261–301.

Bradbury, J.P., Forester, R.M., and Thompson, R.S., 1989, Late Quaternary paleolimnology of Walker Lake, Nevada: Journal of Paleolimnology, v. 1, p. 249–267.

Reno, University of Nevada, unpublished Ph.D. dissertation, 179 p.

Claassen, H.C., 1985, Sources and mechanisms of recharge for ground water in the west-central Amargosa Desert, Nevada—A geochemical interpretation: U.S. Geological Survey Professional Paper 712–F, 31 p.

Coe, J., Glancy, P., and Whitney, J.W., 1995, Volumetric analysis and hydrologic characterization of a modern debris flow near Yucca Mountain, Nevada: U.S. Geological Survey Administrative Report, 50 p.

Coplen, T.B., Winograd, I.J., Landwehr, J.M., and Riggs, A.C., 1994, 500,000-year stable carbon isotopic record from Devils Hole, Nevada: Science, v. 263, p. 361–365.

Cronquist, A., Holmgren, A.H., Holmgren, N.H., and Reveal, J.L., 1972, Intermountain flora—Vascular plants of the intermountain west, U.S.A., volume 1: New York, Hafner Publishing Company, Inc., 270 p.

Czarnecki, J., 1985, Simulated effects of increased recharge on the ground-water flow system of Yucca Mountain and vicinity, Nevada-California: U.S. Geological Survey Water-Resources Investigation Report 84–4344, 33 p.

Delorme, L.D., 1970, Freshwater ostracodes of Canada, Part IV, Families Ilyocyprididae, Notodromadidae, Darwinulidae, Cytherideidae, and Entocytheridae: Canadian Journal of Zoology, v. 48, no. 6, 1251–1259.

Enzel, Y., Cayan, D.R., Anderson, R.Y., and Wells, S.G., 1989, Atmospheric circulation during Holocene lake stands in the Mojave Desert—Evidence of regional climate change: Nature v. 341, p. 44–47.

Eugster, H.P., and Jones, B.F., 1979, Behavior of major solutes during closed-basin brine evolution: American Journal of Science, v. 279, p. 609–631.

rings and climate—Implications for Great Basin paleo-environmental studies, *in* High-Level Radioactive Waste Management, Proceedings of the Fifth International Conference, Las Vegas, Nevada, 1994: LaGrange Park, Illinois, American Nuclear Society, p. 2569–2573.

Grootes, P.M., 1993, Interpreting continental oxygen isotope records, *in* Swart, P.M., Lohmann, P.K., McKenzie, K.C., and Savin, S., eds., Climate change in Continental Isotopic Records: Geophysical Monograph 78, p. 37–46.

Hall, E.R., 1995, Mammals of Nevada (updated edition of the 1946 original): Reno, University of Nevada Press, 710 p.

Ludwig, K.R., Simmons, K.R., Szabo, B.J., Winograd, I.J., Landwehr, J.M., Riggs, A.C., and Hoffman, R.J., 1992, Mass spectrometric ^{230}U–^{234}U–^{238}U dating of the Devils Hole calcite vein: Science, v. 258, p. 284–287.

Ludwig, K.R., Peterman, Z.E., Simmons, K.R., and Gutentag, E.D., 1993, $^{234}U/^{238}U$ ratios as a groundwater flow tracer, southwest Nevada-southeast California, *in* High-Level Radioactive Waste Management, Proceedings of the Fourth International Conference, Las Vegas, Nevada, 1993: LaGrange Park, Illinois, American Nuclear Society, p. 1567–1572.

Lundstrom, S.C., and Taylor, E.M., in press, Preliminary surficial deposits map of the southern half of the Topopah Spring northwest quadrangle: U.S. Geological Survey Open-File Report 95–132, scale 1:12,000.

Preliminary surficial deposits map of the northeast quarter of the Busted Butte 7.5′ quadrangle, Nye County, Nevada: U.S. Geological Survey Open-File Report 94–341.

Lundstrom, S.C., Whitney, J.W., Paces, J.B., Mahan, S.A., and Ludwig, K.R., in press, Preliminary map of the surficial deposits of the southern half of the Busted Butte 7.5′ quadrangle, Nye County, Nevada: U.S. Geological Survey Open-File Report 95–311.

Machette, M.N., 1985, Calcic soils of the southwestern United States: Geological Society of America Special Paper, 203, p. 1–21.

Marshall, B.D., Peterman, Z.E., and Stuckless, J.S., 1993, Strontium isotopic evidence for a higher water table at Yucca Mountain. *in* High Level Radioactive Waste Management, Proceedings of the Fourth International Conference, Las Vegas, Nevada, (DATE): LaGrange Park, Illinois, American Nuclear Society, v. 2, p. 1948-1952.

Marshall, B.D., Peterman, Z.E., and Stuckless, J.S., 1994, Paleohydrology from strontium isotopes at Yucca Mountain, Nevada, *in* Lanphere, M.A., Dalrymple, G.B., and Turrin, B.D., eds., Abstracts of the Eighth International Conference on Geochronology, Cosmochronology, and Isotope Geology: U.S. Geological Survey Circular 1107, p. 203.

Marshall, B.D., Whelan, J.F., Peterman, Z.E., Futa, K., Mahan, S.A., and Stuckless, J.S., 1992, Isotopic studies of fracture coatings at Yucca Mountain, Nevada: Proceedings of the Seventh International Symposium on Water-Rock Interaction, Rotterdam, A.A. Balkema, v. 1, p. 737–740.

Marshall, B.D., and Mahan, S.A., 1994, Strontium-isotope geochemistry of soil and playa deposits near Yucca Mountain, Nevada, *in* High-Level Radioactive Waste Management, Proceedings of the Fifth International Conference, Las Vegas, Nevada, 1994: LaGrange, Illinois, American Nuclear Society, p. 2685–2691.

[illegible] Desert mountain range: Journal of the Arizona Academy of Science 5(4), p. 284–292.

Mehringer, P.J., and Warren, C.N., 1976, Marsh, dune and archaeological chronology, Ash Meadows, Amargosa Desert, Nevada, *in* Elston, R.G., and Headrick, P., eds., Holocene environmental change in the Great Basin, Nevada: Reno, Archeological Survey Research Papers 6, p. 120–150.

Mehringer, P.J., Jr., 1967, Pollen analysis of the Tule Springs area, Nevada, *in* Wormington, H.M., and Ellis, D., eds., Pleistocene studies in southern Nevada: Nevada State Museum, Anthropological Papers 13, p. 131–200.

Menking, K.M., Musler, H.M., Fitts, J.P., Bischoff, J.L., and Anderson, R.S., 1993, Clay mineralogical analyses of the Owens Lake core, *in* Smith, G.I., and Bischoff, J.L., eds., Core OL–92 from Owens Lake, southeast California: U.S. Geological Survey Open-File Report 93–683, p. 75–82.

O'Neil, J.R., Clayton, R.N., and Mayeda T.K., 1969, Oxygen isotope fractionation in divalent metal carbonates: Journal of Chemistry and Physics, v. 51, p. 5547–5558.

Paces, J.B., 1996, Dating of fracture coatings in the ESF: U.S. Geological Survey 1996 Milestone Report DGQH455, 20 p.

Paces, J.B., Menges, C.M., Widmann, B., Wesling, J.R., Bush, C.A., Futa, K., Millard, H.T., Maat, P.B., and Whitney, J.W., 1994, Preliminary U-series disequilibrium and thermoluminescence ages of surficial deposits and paleosols associated with Quaternary faults, eastern Yucca Mountain, *in* High-Level Radioactive Waste Management, Proceedings of the Fifth International Conference, Las Vegas, Nevada, 1994: LaGrange Park, Illinois, American Nuclear Society p. 2391–2401.

Peterman, Z.E., Stuckless, J.S., Marshall, B.D., Mahan, S.A., and Futa, K.A., 1992a, Strontium isotope geochemistry of calcite fracture fillings in deep core, Yucca Mountain, Nevada—A progress report *in* High Level Radioactive Waste Management, Proceedings of the Third International Conference, Las Vegas, Nevada, (DATE): LaGrange, Illinois, American Nuclear Society, p. 1582–1586.

Peterman, Z.E., Stuckless, J.S., Mahan, S.A., Marshall, B.D., Gutentag, E.D., and Downey, J.S., 1992b, Strontium isotope characterization of the Ash Meadows ground-water system, southern Nevada, USA, *in* Kharaka, Y.K., and Maest, A.S., eds., Water-rock interaction—Proceedings of the seventh International Symposium on Water-Rock Interaction: Rotterdam, A.A. Balkema, v. 1, p. 825–829.

Peterman, Z.E., Widmann, B.L., Marshall, B.D., Aleinikoff, J.N., Futa, K., Mahan, S.A., 1994, Isotopic tracers of gold deposition in Paleozoic limestones, southern Nevada *in* High Level Radioactive Waste Management, Proceedings of the Fifth International Conference, Las Vegas, Nevada, (DATE): LaGrange, Illinois, American Nuclear Society, v. 4, p. 1316–1323.

Peterman, Z.E., and Stuckless, J.S., 1993a, Isotopic evidence of complex ground-water flow at Yucca Mountain, Nevada, USA *in* High Level Radioactive Waste Management, Proceedings of the Fourth International Conference, Las Vegas, Nevada, (DATE): LaGrange, Illinois, American Nuclear Society, v. 2, p. 1559–1566.

Peterman, Z.E., and Stuckless, J.S., 1993b, Application of strontium and other radiogenic tracer isotopes to paleohydrologic studies, Paleohydrological Methods and their Applications: Paris, Proceedings of an NEA Workshop, November 1992, p. 59–84.

Pyke, C.B., 1972, Some meteorological aspects of the seasonal distribution of precipitation in the western United States and Baja California: University of California Water Resources Center, Contribution 139, 205 p.

Quade, J., Mifflin, M.D., Pratt, W.L., McCoy, W., and Burckle, L., 1995, Fossil spring deposits in the southern Great Basin and their implications for changes in water-table levels near Yucca Mountain, Nevada, during Quaternary time: Geological Society of America Bulletin, v. 107, p. 213–230.

transects in the southern Great Basin, United States: Geological Society of America Bulletin, v. 101, p. 464–475.

Quade, Jay, 1986, Late Quaternary environmental changes in the upper Las Vegas Valley, Nevada: Quaternary Research, v. 26, no. 3, p. 340–357.

Quade, Jay, and Pratt, W.L., 1989, Late Wisconsin ground-water discharge—Environments of the southwestern Indian Springs Valley, southern Nevada: Quaternary Research, v. 31, no. 3, p. 351–370.

Riggs, A., 1984, Major carbon-14 deficiency in modern snail shells from southern Nevada springs: Science, v. 224, p. 58–61.

Robison, J.H., 1984, Ground-water-level data and preliminary potentiometric-surface maps, Yucca Mountain and vicinity, Nye County, Nevada: U.S. Geological Survey Water-Resources Investigations Report 84–4197.

Roedder, Edwin, Whelan, J.F., and Vaniman, D.T., 1994, Fluid-inclusion homogenization and crushing studies of calcite veins from Yucca Mountain, Nevada, tuffs—Environment of formation *in* High Level Radioactive Waste Management, Proceedings of the Fifth International Conference, Las Vegas, Nevada, (DATE): LaGrange, Illinois, American Nuclear Society, p. 1854–1860.

Sarna-Wojcicki, A.M., Meyer, C.E., Wam, E., and Soles, S., 1993, Age and correlation of tephra layers in Owens Lake drill core OL–92–1 and –2, *in* Smith, G.I., and Bischoff, J.L., eds., Core OL–92 from Owens Lake, southeast California: U.S. Geological Survey Open-File Report 93–683, p. 183–245.

Sass, J.H., Lachenbruch, A.H., and Mase, C.W., 1980, Analysis of thermal data from drill holes UE-25a #3 and UE-25a #1, Calico Hills and Yucca Mountain, Nevada Test Site: U.S. Geological Survey Open-File Report 80–826, 25 p.

Savard, C.S., and Beck, D.A., 1994, Transmission losses in Fortymile Wash near Yucca Mountain, Nevada: Eos, v. 75, no. 44, p. 283.

Smith, G.I., 1976, Paleoclimatic record in the upper Quaternary sediments of Searles Lake, California, U.S.A., *in* Horie, S., ed., Paleolimnology of Lake Biwa and the Japanese Pleistocene 4: Japan, Kyoto University, p. 577–604.

Smith, G.I., 1993, Field log of core OL–92, *in* Smith, G.I., and Bischoff, J.L., eds., Core OL–92 from Owens Lake, southeast California: U.S. Geological Survey Open-File Report 93–683, p. 1–57.

Smith, G.I., and Street-Perrott, F.A., 1983, Pluvial lakes of the western United States, *in* Wright, H.E., ed., Late Quaternary environments of the United States: Minneapolis, University of Minnesota Press, chapter 10, p. 190–212.

Spaulding, W.G., 1977, Late Quaternary vegetation change in the Sheep Range, southern Nevada: Journal of the Arizona Academy of Sciences v. 22, p. 183–188.

Spaulding, W.G., 1981, The late Quaternary vegetation of a southern Nevada mountain range: Tucson, University of Arizona, unpublished Ph.D. dissertation, 271 p.

Spaulding, W.G., 1985, Vegetation and climates of the last 45,000 years in the vicinity of the Nevada Test Site, south-central Nevada: U.S. Geological Survey Professional Paper 1329, 83 p.

Spaulding, W.G., 1990, Vegetational and climatic development of the last glacial maximum to the present, *in* Betancourt, J.L., Van Devender, T.R., and Martin, P.S., eds., Packrat middens—The last 40,000 years of biotic change, chapter 9: Tucson, University of Arizona Press.

Steele, R., 1990, *Pinus flexilis* James Limber Pine, *in* Burns, R. M. and B. H. Honkala (Technical Coordinators), Silvics of North America: Volume 1, Conifers. Agriculture Handbook 654: Forest Service, United States Department of Agriculture, p. 348–354.

Stuiver, M., Long, A., Kra, R.S., and Devine, J.M., 1993, Extended ^{14}C data base and revised CALIB 3.0 ^{14}C age calibration program: Radiocarbon, v. 35, p. 215–230.

Szabo, B.J., and Kyser, T.K., 1990, Ages and stable-isotope compositions of secondary calcite and opal in drill cores from Tertiary volcanic rocks of the Yucca Mountain area, Nevada: Geological Society of America Bulletin, v. 102, p. 1714–1719.

Thompson, R.S., 1991, Pliocene environments and climates in the western United States: Quaternary Science Reviews, v. 10, p. 115–132.

Thompson, R.S., Witlock, C., Bartlein, P.J., Harrison, S.P., and Spaulding, W.G., 1993, Chapter 18: Climatic changes in the western United States since 18,000 yr. B.P., in Wright, H.E., Jr., J.E., Kutzbach, T. Webb III, W.F. Ruddiman, F. a. Street-Perrott and P.J. Barlein (eds.), Global Climates since the Last Glacial Maximum: University of Minnesota Press, Minneapolis, Minnesota, pp. 468–513.

United States Air Force, Headquarters, Tactical Air Command, 1986, Final environmental impact statement, Groom Mountain Range, Lincoln County, Nevada: HQ_TAC/LEEV.

Van Devender, T.R., Martin, P.S., Thompson, R.S., Cole, K.L., Jull, A.J.T., Long, A., Toolin, L.J., and Donahue, D.J., 1986, Fossil packrat middens and the tandem accelerator mass spectrometer: Nature, v. 317, p. 610-613.

Waddell, R.K., Robison, J.H., and Blankennagel, R.K., 1984, Hydrology of Yucca Mountain and vicinity, Nevada-California—Investigative results through mid-1983: U.S. Geological Survey Water-Resources Investigations Report 84–4267, 72 p.

Wells, P.V., and Berger, R., 1967, Late Pleistocene history of coniferous woodland in the Mohave Desert: Science, v. 155, no. 3770, p. 1640–1647.

Wells, P.V., and Jorgensen, C.D, 1964, Pleistocene wood rat middens and climatic change in the Mohave Desert—A record of juniper woodland: Science, v. 143, no. 3611, p. 1171–1174.

Wells, P.V., and Woodcock, D., 1985, Full-glacial vegetation of Death Valley, California—Juniper woodland opening to Yucca semidesert: Madrono, v. 32, p. 11–32.

Whelan, J.F., and Stuckless, J.S., 1990, Reconnaissance $\delta^{13}C$ and $\delta^{18}O$ data from Trench 14, Busted Butte, and drill hole G–4, Yucca Mountain, Nevada Test Site: Las Vegas *in* High Level Radioactive Waste Management, Proceedings of the First International Conference, Las Vegas, Nevada, (DATE): LaGrange, Illinois, American Nuclear Society, p. 930–934.

Whelan, J.F., and Stuckless, J.S., 1992, Paleohydrologic implications of the stable isotopic composition of secondary calcite within the Tertiary volcanic rocks of Yucca Mountain, Nevada: Las Vegas *in* High Level Radioactive Waste Management, Proceedings of the Third International Conference, Las Vegas, Nevada, (DATE): LaGrange, Illinois, American Nuclear Society, p. 1572–1581.

Whelan, J.F., Moscati, R.J., Allerton, S.B.M., and Marshall, B.D., 1996, Applications of isotope geochemistry to the reconstruction of Yucca Mountain paleohydrology: U.S. Geological Survey Milestone Report 3GQH257M to DOE-YMPSCO.

Whelan, J.F., Vaniman, D.T., Stuckless, J.S., and Moscati, R.J., 1994, Paleoclimatic and paleohydrologic records from secondary calcite—Yucca Mountain, Nevada, *in* High-Level Radioactive Waste Management, Proceedings of the Fifth International Conference, Las Vegas, Nevada, 1994: LaGrange, Illinois, American Nuclear Society, p. 2738-2745.

Winograd, I.J., and Doty, G.C., 1980, Paleohydrology of the southern Great Basin with special reference to water-table fluctuations beneath the Nevada Test Site during the late(?) Pleistocene: U.S. Geological Survey Open-File Report 80–569, 91 p.

precipitation to recharge to the Spring Mountains, Nevada, Hydrogeology Journal, v. 6 (1), p. 77–93.

Winograd, I.J., and Szabo, B.J., 1988, Water-table decline in the south-central Great Basin during the Quaternary—Implications for toxic waste disposal, *in* Carr, M.D., and Yount, J.C., eds., Geologic and hydrologic investigations, Yucca Mountain, Nevada: U.S. Geological Survey Bulletin 1790, p. 147–152.

Winograd, I.J., Copeland, T.B., Landwehr, J.M., Riggs, A.C., Ludwig, K.R., Simmons, K.R., Szabo, B.J., Kolesar, P.T., and Revesz, K.M., 1992, Continuous 500,000-year climate record from vein calcite in Devils Hole, Nevada: Science, v. 258, p. 255–284.

deuterium depletion in Great Basin ground waters: Science, v. 227, p. 519–522.

Winograd, I.J., Szabo, B.J., Coplen, T.B., and Riggs, A.C., 1988, A 250,000-year climatic record from Great Basin vein calcite—Implications for Milankovitch Theory: Science, v. 142, p. 1275.

Winter, T.C. and Woo, M.K., 1990, Hydrology of lakes and wetlands, *in* Wolman, M.G., ed., Surface water hydrology, *in the collection* The geology of North America: Boulder, Colo., Geological Society of America, 0-1, chap. 8, p. 159–187.